

Ultrasonic imaging in highly heterogeneous backgrounds

Fatemeh Pourahmadian^{*1,2} and Housseem Haddar³

¹*Department of Civil, Environmental & Architectural Engineering, University of Colorado Boulder, USA*

²*Department of Applied Mathematics, University of Colorado Boulder, USA*

³*INRIA, Center of Saclay Ile de France and UMA, ENSTA Paris Tech, Palaiseau Cedex, FRANCE*

Abstract

This work formally investigates the differential evolution indicators as a tool for ultrasonic tracking of elastic transformation and fracturing in randomly heterogeneous solids. Within the framework of periodic sensing, it is assumed that the background at time t_o contains (i) a multiply connected set of viscoelastic, anisotropic, and piece-wise homogeneous inclusions, and (ii) a union of possibly disjoint fractures and pores. The support, material properties, and interfacial condition of scatterers in (i) and (ii) are unknown, while elastic constants of the matrix are provided. The domain undergoes progressive variations of arbitrary chemo-mechanical origins such that its geometric configuration and elastic properties at future times are distinct. At every sensing step t_o, t_1, \dots , multi-modal incidents are generated by a set of boundary excitations, and the resulting scattered fields are captured over the observation surface. The test data are then used to construct a sequence of wavefront densities by solving the spectral scattering equation. The incident fields affiliated with distinct pairs of obtained wavefronts are analyzed over the stationary and evolving scatterers for a suit of geometric and elastic evolution scenarios entailing both interfacial and volumetric transformations. The main theorem establishes the invariance of pertinent incident fields at the loci of static fractures and inclusions between a given pair of time steps, while certifying variation of the same fields over the modified regions. These results furnish a basis for theoretical justification of differential evolution indicators for imaging in complex composites which, in turn, enable the exclusive tomography of evolution in a background endowed with many unknown features.

1 Introduction

Many critical components in aerospace structures and energy systems are comprised of highly heterogeneous composites [47, 14]. Examples include (a) single- and polycrystalline superalloys deployed in aeroengine and gas turbine blades [9], (b) interpenetrating phase metamaterials such as SiC-SiC composites used in accident-tolerant nuclear fuel claddings [3, 52], and (c) multifunctional polymer matrix composites with a wide spectrum of applications thanks to their

*Corresponding author email: fatemeh.pourahmadian@colorado.edu

exceptional mechanical properties [30, 53]. The topology and characteristics of such materials at micro- and meso- scales are often unknown, or only known to a limited extent because of variabilities in the manufacturing process [41, 45] and/or aging [56]. In addition, mechanisms of deterioration via corrosion, fatigue, irradiation, and thermal cycling are yet to be fully understood. These processes, however, are responsible for continuous microstructural evolution leading to inevitable development of micro/macro cracks and volumetric damage zones which may result in the loss of functional performance in key components [11, 51].

Recent developments in sensing technology have resulted in a suit of imaging solutions germane to complex environments [1, 31, 60, 32, 17, 57, 8, 58]. State-of-the-art examples include: penetrating-radar techniques [1], infrared thermography [31], laser shearography [60], X-ray computed tomography [32], acoustic tomography [17], ultrasonic surface wave methods [57], nonlinear ultrasound [8], and laser ultrasonic imaging [58]. Among which, ultrasonic sensing often emerges as the preferred (or the only feasible) imaging modality in many applications. Laser ultrasonics [55, 59, 29], in particular, has come under the spotlight for enabling non-contact actuation and measurement that is crucial for high-fidelity in-situ monitoring of fabrication processes and advanced manufacturing [61, 58, 39].

Existing approaches to ultrasonic waveform inversion mostly rely on (a) distinct patterns in the measured scattered field associated with certain modes of propagation, (b) specific sensing configurations, and (c) major postulates on the nature of wave motion in the background which, by and large, forgo the uncertain (yet important) scattering signatures affiliated with the specimen's microstructure. Such attributes expedite the data processing, yet entail the following impediments: (i) unstable reconstructions featuring many artifacts, (ii) significant errors in heterogeneous and anisotropic backgrounds where multiple scattering generates remarkable wave dispersion and attenuation, (iii) major restrictions on the geometry of incident and/or measurement grids, (iv) limited scalability beyond the controlled laboratory environment. Thus, there is a critical need for next-generation imaging solutions that carefully integrate state-of-the-art instrumentation and advanced data analytic solutions to enable fast (yet robust) ultrasonic tomography of complex processes in uncertain or unknown environments.

Ongoing efforts in this vein are mainly focused on (a) optimization-based full-waveform inversion, and (b) machine learning (ML). Inverse algorithms in (a) have so far been associated with tardy reconstructions due to their high computational cost. Lately, a few studies showed that the latter may be addressed by leveraging deep learning solutions pertinent to partial differential equations such as physics-informed neural networks [27, 26]. However, the majority of paradigms in (b) make use of ML principles within the framework of existing logics for ultrasonic imaging so that the above-mentioned barriers are not fundamentally resolved. Nonetheless, ML schemes are shown to facilitate the implementation of various imaging solutions, and may serve as effective post-processing tools for image enhancement [54, 21, 2].

In applied mathematics, in parallel, over two decades of research in inverse scattering and transmission eigenvalues has given rise to a suit of rigorous algorithms for non-iterative waveform inversion [19, 18, 7, 34, 16]. Recently, sampling-based approaches to inverse scattering have

been applied to laser-ultrasonic test data [44]. The results demonstrate superior reconstructions in terms of quality and resolution compared to conventional methods. In addition, introduction of the differential evolution indicators [6] as a tool for waveform tomography in unknown media showcase a unique opportunity to achieve the above-mentioned goal for real-time, laser-based monitoring. The differential indicators have so far been theoretically established for (i) acoustic imaging of obstacles in periodic and random media [46, 5], and (ii) elastic-wave imaging of fractures in monolithic solids [50, 48]. A rigorous justification of this imaging modality for its potentially dominant field of application i.e., ultrasonic tomography in complex composites – where the background features a random distribution of heterogeneities and discontinuities of unknown support and material characteristics which are subject to both interfacial and volumetric evolution, is still lacking. The present study is an effort toward establishing the differential evolution indicators in the general case of solids. In this vein, a special attention is paid to pose the forward scattering problem in a broad sense by taking advantage of contributions on the nature of transmission eigenvalues in elastodynamics [22, 24, 23, 25, 13, 12, 20].

More specifically, the direct problem formulates sequential experiments conducted on a randomly structured composite such that at every sensing step t_0, t_1, \dots , the specimen features an arbitrary networks of pores and fractures along with a set of viscoelastic, anisotropic, and heterogeneous inclusions embedded in an elastic matrix. Properties of the binder are assumed to be known, while the support, material properties, and interfacial condition of scatterers are a-priori unknown and subject to spatiotemporal evolution. In this setting, boundary excitations at every time step give rise to distinct scattering footprints on the measurement surface. The idea is to use the sequence of scattered field measurements to design an imaging functional endowed with appropriate invariance with respect to stationary scatterers between any pairs of time steps such that the associated reconstructions uniquely expose the support of mechanical evolution in a given timeframe without the need to image the entire domain which may be insurmountable. To this end, the conditions for wellposedness of the forward problem are identified. The set of spectral scattering equations is then defined for waveform inversion. At every time step, the affiliated scattering operator and its related properties are carefully analyzed in order to construct a sequence of approximate solutions to the scattering equation with strong convergence characteristics under a certain condition. The obtained solutions i.e., wavefront densities are then used to specify a set of incident fields over a generic model of the background, which forms the basis for differential imaging indicators. Next, the incidents corresponding to distinct pairs of wavefronts are analyzed over the stationary and evolving scatterers for a suit of geometric and elastic evolution configurations. In the general case of solids, the latter involves a number of novel scenarios including (a) fracturing at bimaterial interfaces, (b) elastic transformation and/or expansion of fractured inclusions, and (c) elastic conversion of microcracked damage zones. The main theorem establishes the invariance of incident fields at the loci of stationary fractures and inclusions, while certifying variation of the same fields over the evolved regions. These results pave the way for differential tomography of evolution in unknown backgrounds.

In the sequel, Section 2 provides the geometric and mechanistic description of the direct scattering problem. Section 3 specifies the fundamental properties of scattering operators. The main theorems in Section 5 establish the behavior of differential indicators in the case of composites. Section 6 is dedicated to a numerical implementation and discussion of the results.

2 Preliminaries

Consider periodic illumination of mechanical evolution in a randomly structured composite shown in Fig. (1). At the first sensing step $t = t_0$, the specimen $\mathcal{B} \subset \mathbb{R}^3$ is comprised of (i) a linear, elastic, isotropic and homogeneous binder of mass density $\rho \in \mathbb{R}$ and Lamé parameters $\mu, \lambda \in \mathbb{R}$, (ii) a union of bounded inclusions $\mathcal{D}_\circ^* \cup \mathcal{D}_\circ^o = \mathcal{D}_\circ \subset \mathcal{B}$ with Lipschitz boundaries composed of penetrable \mathcal{D}_\circ^* and impenetrable \mathcal{D}_\circ^o components where in the former case, the inclusions may be viscoelastic, anisotropic, and multiply connected, and (iii) a network of discontinuity surfaces $\Gamma_\circ \subset \mathcal{B}$ characterized by the complex-valued and heterogeneous interfacial stiffness matrix $\mathbf{K}_\circ(\boldsymbol{\xi})$ where $\boldsymbol{\xi} \in \Gamma_\circ$ is the position vector. The specimen may be exposed to irradiation or chemical reactions as common producers of interfacial damage [37], and/or subject to thermal cycling, fatigue, and shock-waves which are mostly responsible for volumetric degradation [38] so that at any future sensing steps $t = t_i > t_0$, $i \in \mathbb{N}$, the domain \mathcal{B} features an evolved set of inclusions $\mathcal{D}_i^* \cup \mathcal{D}_i^o = \mathcal{D}_i \subset \mathcal{B}$ and interfaces $\Gamma_i \subset \mathcal{B}$ such that $\mathcal{D}_{i-1} \subset \mathcal{D}_i$ and $\Gamma_{i-1} \setminus \overline{\mathcal{D}_i^o} \subset \Gamma_i$, $\forall i \in \mathbb{N}$. For further clarity, let $\rho_\kappa = \rho_\kappa(\boldsymbol{\xi}) > 0$ and $\mathbf{C}_\kappa = \mathbf{C}_\kappa(\boldsymbol{\xi})$, $\kappa = \circ, 1, \dots$, designate the mass density and (complex-valued) viscoelasticity tensor associated with the penetrable obstacles \mathcal{D}_κ^* at t_κ . Here, $(\mathbf{C}_\kappa, \rho_\kappa)$ are understood in a piecewise-constant sense i.e., \mathcal{D}_κ^* can be decomposed into N_κ open, simply connected, and non-overlapping subsets $\mathcal{D}_\kappa^n \subset \mathcal{D}_\kappa^*$ (of Lipschitz boundaries) where both ρ_κ and \mathbf{C}_κ are constants $\forall \boldsymbol{\xi} \in \mathcal{D}_\kappa^n$, and $\overline{\mathcal{D}_\kappa^*} = \bigcup_{n=1}^{N_\kappa} \overline{\mathcal{D}_\kappa^n}$. It should be noted that $\forall t_\kappa$, \mathcal{D}_κ^* and \mathcal{D}_κ^o are assumed to be disjoint i.e., $\overline{\mathcal{D}_\kappa^*} \cap \overline{\mathcal{D}_\kappa^o} = \emptyset$. In addition, the support of Γ_κ may be decomposed into N_κ smooth open subsets $\Gamma_n \subset \Gamma_\kappa$, $n = 1, \dots, N_\kappa$, such that $\Gamma_\kappa = \bigcup_{n=1}^{N_\kappa} \Gamma_n$. The support of Γ_n may be arbitrarily extended to a closed Lipschitz surface ∂D_n of a bounded simply connected domain D_n , so that the unit normal vector \mathbf{n} to Γ_n coincides with the outward normal vector to ∂D_n . We assume that Γ_n is an open set (relative to ∂D_n) with a positive surface measure.

In this setting, let $\mathcal{E}_i^* \cup \mathcal{E}_i^o$ and $\hat{\Gamma}_i \cup \tilde{\Gamma}_i$ respectively specify the support of volumetric and interfacial evolution within $[t_{i-1}, t_i]$ for $i \in \mathbb{N}$ such that

$$\begin{aligned} \overline{\hat{\Gamma}_i} &:= \overline{\Gamma_i \setminus \overline{\Gamma_{i-1}}}, & \overline{\tilde{\Gamma}_i} &:= \overline{\{\boldsymbol{\xi} \in \Gamma_{i-1} \setminus \overline{\mathcal{D}_i^o} : \mathbf{K}_{i-1}(\boldsymbol{\xi}) \neq \mathbf{K}_i(\boldsymbol{\xi})\}}, \\ \overline{\mathcal{E}_i^o} &:= \overline{\mathcal{D}_i^o \setminus \overline{\mathcal{D}_{i-1}^o}}, & \overline{\mathcal{E}_i^*} &:= \overline{\text{supp}(\mathbf{C}_i - \mathbf{C}_{i-1}) \cup \text{supp}(\rho_i - \rho_{i-1})}, \quad i = 1, 2, \dots \end{aligned} \quad (1)$$

At $t = t_0$, the specimen's external boundary $\partial \mathcal{B}$ and the binder's constants (λ, μ, ρ) are known which may be used to define a *baseline model* of the background. On the other hand, the support of pre-existing scatterers $\mathcal{D}_\circ \cup \Gamma_\circ$ and their designated properties $(\mathbf{C}_\circ, \rho_\circ, \mathbf{K}_\circ)(\boldsymbol{\xi})$ are unknown. Given sequential sensory data at t_{i-1} and t_i for $i \in \mathbb{N}$, the objective is to reconstruct the support of volumetric and interfacial evolution $\mathcal{E}_i^* \cup \mathcal{E}_i^o \cup \hat{\Gamma}_i \cup \tilde{\Gamma}_i$ defined by (1).

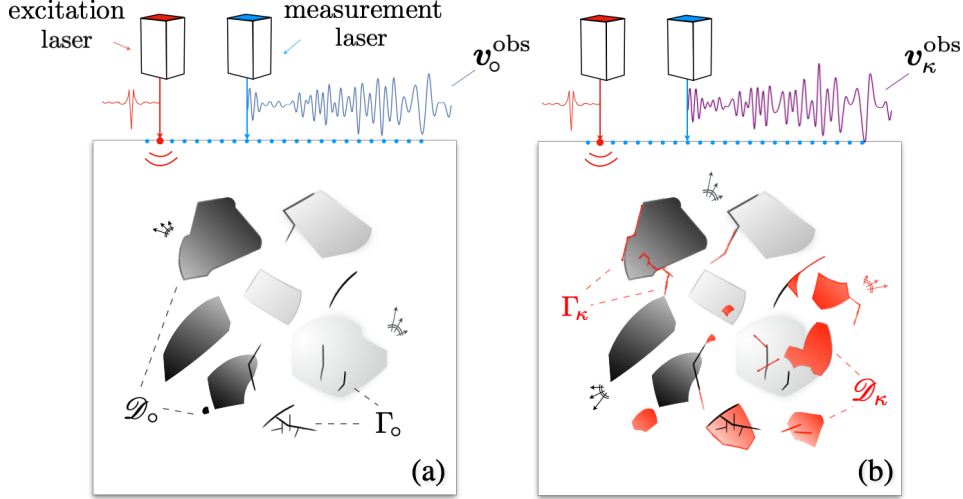


Figure 1: Ultrasonic sensing of evolution in a heterogeneous composite featuring a network of arbitrary inclusions, fractures, and pores of unknown distribution, elastic properties, and interfacial conditions: **(a)** *primary experiments* conducted at $t = t_o$ when a set of boundary excitations, interacting with the unknown pre-existing scatterers $\mathcal{D}_o \cup \Gamma_o$, induce the scattered field $\mathbf{v}_o^{\text{obs}}$ on the observation surface, and **(b)** *secondary experiments* performed sequentially at later times $t_i = \{t_1, t_2, \dots\}$ when new and evolved scatterers $\mathcal{D}_\kappa \cup \Gamma_\kappa$ lead to distinct waveform measurements $\mathbf{v}_\kappa^{\text{obs}}$.

Assumption 2.1. Let $\Gamma_\kappa^o \subset \Gamma_\kappa$ denote the union of traction-free cracks at t_κ such that

$$\overline{\Gamma_\kappa^o} := \overline{\{\boldsymbol{\xi} \in \Gamma_\kappa : \mathbf{K}_\kappa(\boldsymbol{\xi}) = \mathbf{0}\}}, \quad \kappa = o, 1, \dots,$$

then $\mathcal{B} \setminus \overline{\mathcal{D}_\kappa^o \cup \Gamma_\kappa^o}$ remains connected $\forall t_\kappa$.

Assumption 2.2. Let $\Re(\cdot)$ and $\Im(\cdot)$ respectively denote the real and imaginary parts of a complex-valued quantity, and recall that the fourth-order tensor $\mathbf{C}_\kappa(\boldsymbol{\xi})$ represents the viscoelastic and anisotropic behavior of inclusions \mathcal{D}_κ^* at t_κ . Then, the real part of \mathbf{C}_κ is bounded by piecewise-constant and strictly positive functions \mathbf{c}_κ and \mathbf{C}_κ , while the magnitude of its imaginary part is constrained by piecewise-constant and non-negative functions \mathbf{v}_κ and \mathbf{V}_κ such that $\forall \boldsymbol{\Phi} \in \mathbb{C}(\mathcal{D}_\kappa^*)^{3 \times 3}$,

$$\begin{cases} \mathbf{c}_\kappa |\boldsymbol{\Phi}|^2 \leq \Re(\boldsymbol{\Phi} : \mathbf{C}_\kappa : \overline{\boldsymbol{\Phi}}) \leq \mathbf{C}_\kappa |\boldsymbol{\Phi}|^2 & \text{in } \mathcal{D}_\kappa^* \\ \mathbf{v}_\kappa |\boldsymbol{\Phi}|^2 \leq -\Im(\boldsymbol{\Phi} : \mathbf{C}_\kappa : \overline{\boldsymbol{\Phi}}) \leq \mathbf{V}_\kappa |\boldsymbol{\Phi}|^2 & \text{in } \mathcal{D}_\kappa^* \end{cases}, \quad \kappa = o, 1, \dots \quad (2)$$

Also, the interfacial stiffness matrix $\mathbf{K}_\kappa \in L^\infty(\Gamma_\kappa)^{3 \times 3}$ is symmetric $\forall \kappa$, while satisfying $\overline{\boldsymbol{\varphi}} \cdot \Im \mathbf{K}_\kappa(\boldsymbol{\xi}) \cdot \boldsymbol{\varphi} \leq 0$, $\forall \boldsymbol{\varphi} \in \mathbb{C}(\Gamma_\kappa)^3$.

Assumption 2.3. Let $\mathbf{C} = \lambda \mathbf{I}_2 \otimes \mathbf{I}_2 + 2\mu \mathbf{I}_4$ denote the binder's fourth-order elasticity tensor, wherein \mathbf{I}_m ($m = 2, 4$) designates the m th-order symmetric identity tensor. Then, given the

Poisson's ratio $\nu = \frac{\lambda}{2(\lambda+\mu)}$ and $\mathcal{B}_\kappa^- := \mathcal{B} \setminus \overline{\mathcal{D}_\kappa \cup \Gamma_\kappa}$, observe that $\forall \Psi \in \mathbb{C}(\mathcal{B}_\kappa^-)^{3 \times 3}$,

$$\begin{cases} 2\mu|\Psi|^2 \leq \Re(\Psi : \mathbf{C} : \overline{\Psi}) \leq (3\lambda + 2\mu)|\Psi|^2 & \text{for } 0 < \nu < \frac{1}{2} \\ (3\lambda + 2\mu)|\Psi|^2 \leq \Re(\Psi : \mathbf{C} : \overline{\Psi}) \leq 2\mu|\Psi|^2 & \text{for } -1 < \nu < 0 \end{cases}, \quad \Im(\Psi : \mathbf{C} : \overline{\Psi}) = 0.$$

Next, invoke $\mathcal{D}_\kappa^n \subset \mathcal{D}_\kappa^*$ with constant $(\mathbf{C}_\kappa, \rho_\kappa)$, and let $\mathbf{c}_\kappa^n, \mathbf{C}_\kappa^n, \mathbf{v}_\kappa^n$, and \mathbf{V}_κ^n represent the respective values of $\mathbf{c}_\kappa, \mathbf{C}_\kappa, \mathbf{v}_\kappa$, and \mathbf{V}_κ in each \mathcal{D}_κ^n , $n \in \{1, \dots, N_\kappa^*\}$ and $\kappa \in \{\circ, 1, \dots\}$. Then, in light of [13], $\forall \kappa$

$$(\rho < \rho_\kappa \wedge \max\{3\lambda + 2\mu, 2\mu\} < \min\{\mathbf{c}_\kappa^n\}) \vee (\rho > \rho_\kappa \wedge \min\{3\lambda + 2\mu, 2\mu\} > \max\{\mathbf{c}_\kappa^n\}).$$

Experiments. The domain \mathcal{B} is subject to periodic inspections at time steps $t_\kappa = \{t_\circ, t_1, \dots\}$. At every t_κ , the specimen is excited by a combination of ultrasonic sources on its external boundary $\partial\mathcal{B}_t$ so that the corresponding incident field $\mathbf{u}^f \in H^1(\mathcal{B})^3$ in the baseline model is governed by

$$\begin{aligned} \nabla \cdot \mathbf{C} : \nabla \mathbf{u}^f(\boldsymbol{\xi}) + \rho\omega^2 \mathbf{u}^f(\boldsymbol{\xi}) &= \mathbf{0}, & \boldsymbol{\xi} \in \mathcal{B}, \\ \mathbf{n} \cdot \mathbf{C} : \nabla \mathbf{u}^f(\boldsymbol{\xi}) &= \boldsymbol{\tau}(\boldsymbol{\xi}), & \boldsymbol{\xi} \in \partial\mathcal{B}_t, \\ \mathbf{u}^f(\boldsymbol{\xi}) &= \mathbf{0}, & \boldsymbol{\xi} \in \partial\mathcal{B} \setminus \partial\mathcal{B}_t. \end{aligned} \quad (3)$$

Here, the illumination frequency $\omega > 0$ is selected such that the shear wavelength $\lambda_s = 2\pi\sqrt{\mu/(\rho\omega^2)}$ is sufficiently smaller than the characteristic length scale of the sought-for objects; \mathbf{n} is the unit outward normal to the sample's boundary $\partial\mathcal{B}$; $\boldsymbol{\tau}(\boldsymbol{\xi})$ represents the external traction on the Neumann part of the boundary $\partial\mathcal{B}_t \subset \partial\mathcal{B}$ which includes the source input. It is assumed that $\text{supp}(\partial\mathcal{B} \setminus \partial\mathcal{B}_t) = \emptyset$, i.e., a set of fixed boundary points of zero surface measure prevent the rigid body motion. Henceforth, the homogeneous Dirichlet part of the boundary will be implicitly indicated. At every sensing step t_κ , the interaction of \mathbf{u}^f with the hidden scatterers $\Gamma_\kappa \cup \mathcal{D}_\kappa$ gives rise to the total field $(\mathbf{u}^\kappa, \mathbf{w}^\kappa) \in H^1(\mathcal{B}_\kappa^-)^3 \times H^1(\mathcal{D}_\kappa^* \setminus \overline{\Gamma_\kappa})^3$ satisfying

$$\begin{aligned} \nabla \cdot \mathbf{C} : \nabla \mathbf{u}^\kappa(\boldsymbol{\xi}) + \rho\omega^2 \mathbf{u}^\kappa(\boldsymbol{\xi}) &= \mathbf{0}, & \boldsymbol{\xi} \in \mathcal{B}_\kappa^-, \\ \nabla \cdot [\mathbf{C}_\kappa(\boldsymbol{\xi}) : \nabla \mathbf{w}^\kappa](\boldsymbol{\xi}) + \rho_\kappa(\boldsymbol{\xi})\omega^2 \mathbf{w}^\kappa(\boldsymbol{\xi}) &= \mathbf{0}, & \boldsymbol{\xi} \in \mathcal{D}_\kappa^* \setminus \overline{\Gamma_\kappa}, \\ \mathbf{t}[\mathbf{u}^\kappa](\boldsymbol{\xi}) = \mathbf{t}[\mathbf{w}^\kappa](\boldsymbol{\xi}), \quad \mathbf{u}^\kappa(\boldsymbol{\xi}) = \mathbf{w}^\kappa(\boldsymbol{\xi}), & & \boldsymbol{\xi} \in \partial\mathcal{D}_\kappa^* \setminus \overline{\Gamma_\kappa}, \\ \mathbf{t}[\mathbf{u}](\boldsymbol{\xi}) = \mathbf{K}_\kappa(\boldsymbol{\xi})[\mathbf{u}](\boldsymbol{\xi}), \quad \llbracket \mathbf{t}[\mathbf{u}] \rrbracket(\boldsymbol{\xi}) &= \mathbf{0}, & \boldsymbol{\xi} \in \Gamma_\kappa, \\ \mathbf{t}[\mathbf{u}^\kappa](\boldsymbol{\xi}) &= \mathbf{0}, & \boldsymbol{\xi} \in \partial\mathcal{D}_\kappa^\circ, \\ \mathbf{t}[\mathbf{u}^\kappa](\boldsymbol{\xi}) &= \boldsymbol{\tau}(\boldsymbol{\xi}), & \boldsymbol{\xi} \in \partial\mathcal{B}_t. \end{aligned} \quad (4)$$

Here,

$$\begin{cases} \mathbf{t}[\mathbf{u}^\kappa](\boldsymbol{\xi}) = \mathbf{n}(\boldsymbol{\xi}) \cdot \mathbf{C} : \nabla \mathbf{u}^\kappa(\boldsymbol{\xi}), & \boldsymbol{\xi} \in \partial\mathcal{B}_t \cup \partial\mathcal{D}_\kappa \\ \mathbf{t}[\mathbf{w}^\kappa](\boldsymbol{\xi}) = \mathbf{n}(\boldsymbol{\xi}) \cdot \mathbf{C}_\kappa(\boldsymbol{\xi}) : \nabla \mathbf{w}^\kappa(\boldsymbol{\xi}), & \boldsymbol{\xi} \in \partial\mathcal{D}_\kappa^* \end{cases},$$

wherein \mathbf{n} is the unit outward normal to $\partial\mathcal{B}$ and $\partial\mathcal{D}_\kappa$. In addition, $\llbracket \mathbf{u} \rrbracket$ (resp. $\llbracket \mathbf{t}[\mathbf{u}] \rrbracket$) denotes

the jump in displacement \mathbf{u} (*resp.* traction $\mathbf{t}[\mathbf{u}]$) across Γ_κ such that

$$\llbracket \mathbf{u} \rrbracket = \begin{cases} \llbracket \mathbf{u}^\kappa \rrbracket & \text{on } \Gamma_\kappa \setminus \overline{\mathcal{D}_\kappa^*} \\ \llbracket \mathbf{w}^\kappa \rrbracket & \text{on } \Gamma_\kappa \cap \mathcal{D}_\kappa^*, \\ \mathbf{u}^\kappa - \mathbf{w}^\kappa & \text{on } \Gamma_\kappa \cap \partial \mathcal{D}_\kappa^* \end{cases}, \quad \llbracket \mathbf{t}[\mathbf{u}] \rrbracket = \begin{cases} \llbracket \mathbf{t}[\mathbf{u}^\kappa] \rrbracket := \llbracket \mathbf{n} \cdot \mathbf{C} : \nabla \mathbf{u}^\kappa \rrbracket & \text{on } \Gamma_\kappa \setminus \overline{\mathcal{D}_\kappa^*} \\ \llbracket \mathbf{t}[\mathbf{w}^\kappa] \rrbracket := \llbracket \mathbf{n} \cdot \mathbf{C}_\kappa : \nabla \mathbf{w}^\kappa \rrbracket & \text{on } \Gamma_\kappa \cap \mathcal{D}_\kappa^*, \\ \mathbf{n} \cdot (\mathbf{C} : \nabla \mathbf{u}^\kappa - \mathbf{C}_\kappa : \nabla \mathbf{w}^\kappa) & \text{on } \Gamma_\kappa \cap \partial \mathcal{D}_\kappa^* \end{cases}$$

where

$$\llbracket \mathbf{f} \rrbracket = \mathbf{f}^+ - \mathbf{f}^-, \quad \mathbf{f}^\pm(\boldsymbol{\xi}) = \lim_{h \rightarrow 0^+} \mathbf{f}(\boldsymbol{\xi} \pm h \mathbf{n}(\boldsymbol{\xi})), \quad \boldsymbol{\xi} \in \Gamma_\kappa.$$

Keep in mind that the unit normal vector \mathbf{n} to Γ_κ is specified earlier. Also, the second of (4) should be understood as a shorthand for the set of N_κ^* governing equations over the respective homogeneous regions \mathcal{D}_κ^n ($n = 1, \dots, N_\kappa^*$), supplemented by the continuity conditions for displacement and traction across $\partial \mathcal{D}_\kappa^n$ as applicable.

Assumption 2.4. $\omega > 0$ is not an eigenvalue of the homogeneous form of (3) and (4).

Given (3) and (4), the scattered field $\mathbf{v}^\kappa \in H^1(\mathcal{B}_\kappa^- \cup \mathcal{D}_\kappa^* \setminus \overline{\Gamma_\kappa})^3$ is governed by

$$\begin{aligned} \nabla \cdot \mathbf{C} : \nabla \mathbf{v}^\kappa(\boldsymbol{\xi}) + \rho \omega^2 \mathbf{v}^\kappa(\boldsymbol{\xi}) + \mathbf{1}(\mathcal{D}_\kappa^* \setminus \overline{\Gamma_\kappa})[\mathbf{f}_\kappa + \nabla \cdot \boldsymbol{\sigma}_\kappa](\boldsymbol{\xi}) &= \mathbf{0}, & \boldsymbol{\xi} \in \mathcal{B}_\kappa^- \cup \mathcal{D}_\kappa^* \setminus \overline{\Gamma_\kappa}, \\ \mathbf{t}[\mathbf{v}^\kappa](\boldsymbol{\xi}) + \mathbf{1}(\overline{\mathcal{D}_\kappa^*} \cap \Gamma_\kappa) \mathbf{n} \cdot \boldsymbol{\sigma}_\kappa(\boldsymbol{\xi}) &= \mathbf{K}_\kappa(\boldsymbol{\xi})[\mathbf{v}^\kappa](\boldsymbol{\xi}) - \mathbf{t}^f(\boldsymbol{\xi}), & \boldsymbol{\xi} \in \Gamma_\kappa, \\ \llbracket \mathbf{t}[\mathbf{v}^\kappa] \rrbracket + \mathbf{1}(\mathcal{D}_\kappa^* \cap \Gamma_\kappa) \mathbf{n} \cdot \boldsymbol{\sigma}_\kappa(\boldsymbol{\xi}) &= \mathbf{1}(\partial \mathcal{D}_\kappa^* \cap \Gamma_\kappa) \mathbf{n} \cdot \boldsymbol{\sigma}_\kappa(\boldsymbol{\xi}), & \boldsymbol{\xi} \in \Gamma_\kappa, \\ \llbracket \mathbf{t}[\mathbf{v}^\kappa] \rrbracket(\boldsymbol{\xi}) &= \mathbf{n} \cdot \boldsymbol{\sigma}_\kappa(\boldsymbol{\xi}), \quad \llbracket \mathbf{v}^\kappa \rrbracket(\boldsymbol{\xi}) = \mathbf{0}, & \boldsymbol{\xi} \in \partial \mathcal{D}_\kappa^* \setminus \overline{\Gamma_\kappa}, \\ \mathbf{t}[\mathbf{v}^\kappa](\boldsymbol{\xi}) &= -\mathbf{t}^f(\boldsymbol{\xi}), & \boldsymbol{\xi} \in \partial \mathcal{D}_\kappa^o, \\ \mathbf{t}[\mathbf{v}^\kappa](\boldsymbol{\xi}) &= \mathbf{0}, & \boldsymbol{\xi} \in \partial \mathcal{B}_t. \end{aligned} \tag{5}$$

where $\mathbf{t}^f := \mathbf{n} \cdot \mathbf{C} : \nabla \mathbf{u}^f$; $\mathbf{t}[\mathbf{v}^\kappa] = \mathbf{t}^-[\mathbf{v}^\kappa] := \mathbf{n} \cdot \mathbf{C} : \nabla \mathbf{v}^{\kappa^-}$; and,

$$\mathbf{f}_\kappa(\boldsymbol{\xi}) := (\rho_\kappa(\boldsymbol{\xi}) - \rho) \omega^2 \mathbf{w}^\kappa(\boldsymbol{\xi}), \quad \boldsymbol{\sigma}_\kappa(\boldsymbol{\xi}) := (\mathbf{C}_\kappa(\boldsymbol{\xi}) - \mathbf{C}) : \nabla \mathbf{w}^\kappa(\boldsymbol{\xi}), \quad \boldsymbol{\xi} \in \mathcal{D}_\kappa^* \setminus \overline{\Gamma_\kappa}.$$

Dimensional platform. In what follows, all quantities are rendered dimensionless by taking ρ , μ , and ℓ_o – denoting the minimum length scale attributed to the hidden scatterers, as the respective reference scales for mass density, elastic modulus, and length – which amounts to setting $\rho = \mu = \ell_o = 1$ [10].

Function spaces. It is known that stress singularities at the branch points of multiple intersecting fractures in an isotropic and homogeneous background is weaker than the classical crack-tip singularity [40, 28]. The latter is also the case for delamination cracks propagating along bi-material interfaces [43]. High-order singularities may occur when a crack tip meets a bi-material interface in an angle [33, 42], in which case it is shown that the contact laws in the vicinity of the crack tip may be modified such that the usual asymptotic forms for stress still applies [4]. In light of this, it will be assumed that $\llbracket \mathbf{u} \rrbracket \in \tilde{H}^{\frac{1}{2}}(\Gamma_\kappa)^3$ where

$$\begin{aligned} H^{\pm \frac{1}{2}}(\Gamma_\kappa)^3 &:= \{ \mathbf{f}|_{\Gamma_\kappa} : \mathbf{f} \in H^{\pm \frac{1}{2}}(\partial D)^3 \}, \\ \tilde{H}^{\pm \frac{1}{2}}(\Gamma_\kappa)^3 &:= \{ \mathbf{f} \in H^{\pm \frac{1}{2}}(\partial D)^3 : \text{supp}(\mathbf{f}) \subset \overline{\Gamma_\kappa} \}. \end{aligned} \tag{6}$$

Here, $D = \bigcup_{n=1}^{N_\kappa} D_n$ is a multiply connected Lipschitz domain of bounded support such that $\Gamma_\kappa \subset \partial D$. Recall that D_n is an arbitrary extension of Γ_n defined in the above. On invoking $H^{-1/2}(\Gamma_\kappa)^3$ and $\tilde{H}^{-1/2}(\Gamma_\kappa)^3$ as the respective dual spaces of $\tilde{H}^{1/2}(\Gamma_\kappa)^3$ and $H^{1/2}(\Gamma_\kappa)^3$, it follows that

$$\tilde{H}^{\frac{1}{2}}(\Gamma_\kappa)^3 \subset H^{\frac{1}{2}}(\Gamma_\kappa)^3 \subset L^2(\Gamma_\kappa)^3 \subset \tilde{H}^{-\frac{1}{2}}(\Gamma_\kappa)^3 \subset H^{-\frac{1}{2}}(\Gamma_\kappa)^3. \quad (7)$$

In this setting, $\mathbf{t}[\mathbf{u}] \in H^{-1/2}(\Gamma_\kappa)^3$. For future reference, let us also define

$$\begin{aligned} S(\mathcal{D}_\kappa^* \cup \Gamma_\kappa \cup \partial \mathcal{D}_\kappa^o) &:= L^2(\mathcal{D}_\kappa^* \setminus \overline{\Gamma_\kappa})^3 \times L^2(\mathcal{D}_\kappa^* \setminus \overline{\Gamma_\kappa})^{3 \times 3} \times H^{-\frac{1}{2}}(\Gamma_\kappa)^3 \times H^{-\frac{1}{2}}(\partial \mathcal{D}_\kappa^o)^3, \\ \tilde{S}(\mathcal{D}_\kappa^* \cup \Gamma_\kappa \cup \partial \mathcal{D}_\kappa^o) &:= L^2(\mathcal{D}_\kappa^* \setminus \overline{\Gamma_\kappa})^3 \times L^2(\mathcal{D}_\kappa^* \setminus \overline{\Gamma_\kappa})^{3 \times 3} \times \tilde{H}^{\frac{1}{2}}(\Gamma_\kappa)^3 \times \tilde{H}^{\frac{1}{2}}(\partial \mathcal{D}_\kappa^o)^3. \end{aligned} \quad (8)$$

Wellposedness. Under Assumptions 2.1 and 2.2, observe that the direct scattering problem (5) is of Fredholm type, and thus, its wellposedness may be established by drawing from the unique continuation principles. See Appendix A for details.

Scattering signatures. By deploying Betti's reciprocal theorem, one obtains the following integral representation for the scattered fields $\mathbf{v}^\kappa := \mathbf{u}^\kappa - \mathbf{u}^f$, $\kappa = \{\circ, 1, 2, \dots\}$, on the specimen's boundary.

$$\begin{aligned} \frac{1}{2} \mathbf{v}^\kappa(\boldsymbol{\xi}) &= \int_{\mathcal{D}_\kappa^* \setminus \overline{\Gamma_\kappa}} [(\rho_\kappa(\mathbf{y}) - \rho) \omega^2 \mathbf{w}^\kappa(\mathbf{y}) \cdot \mathbf{G}(\boldsymbol{\xi}, \mathbf{y}) - \nabla \mathbf{G}(\boldsymbol{\xi}, \mathbf{y}) : (\mathbf{C}_\kappa(\mathbf{y}) - \mathbf{C}) : \nabla \mathbf{w}^\kappa(\mathbf{y})] dV_{\mathbf{y}} + \\ &\int_{\partial \mathcal{D}_\kappa^o} \mathbf{u}^\kappa(\mathbf{y}) \cdot \mathbf{T}(\boldsymbol{\xi}, \mathbf{y}) dS_{\mathbf{y}} + \int_{\Gamma_\kappa} [\mathbf{u}] (\mathbf{y}) \cdot \mathbf{T}(\boldsymbol{\xi}, \mathbf{y}) dS_{\mathbf{y}}, \quad \mathbf{T}(\boldsymbol{\xi}, \mathbf{y}) := \mathbf{n}(\mathbf{y}) \cdot \boldsymbol{\Sigma}(\boldsymbol{\xi}, \mathbf{y}), \quad \boldsymbol{\xi} \in \partial \mathcal{B}_t. \end{aligned} \quad (9)$$

Here, $\mathbf{G}(\boldsymbol{\xi}, \mathbf{y})$ is the Green's displacement tensor solving

$$\begin{aligned} \nabla_{\mathbf{y}} \cdot \mathbf{C} : \nabla_{\mathbf{y}} \mathbf{G}(\boldsymbol{\xi}, \mathbf{y}) + \rho \omega^2 \mathbf{G}(\boldsymbol{\xi}, \mathbf{y}) + \delta(\mathbf{y} - \boldsymbol{\xi}) \mathbf{I}_{3 \times 3} &= \mathbf{0}, & \mathbf{y} \in \mathcal{B} \setminus \{\boldsymbol{\xi}\}, \\ \mathbf{n} \cdot \mathbf{C} : \nabla_{\mathbf{y}} \mathbf{G}(\boldsymbol{\xi}, \mathbf{y}) &= \mathbf{0}, & \mathbf{y} \in \partial \mathcal{B}_t, \end{aligned} \quad (10)$$

and $\boldsymbol{\Sigma}(\boldsymbol{\xi}, \mathbf{y}) := \mathbf{C} : \nabla_{\mathbf{y}} \mathbf{G}(\boldsymbol{\xi}, \mathbf{y})$ is the associated Green's stress tensor.

3 Scattering operators

Let us define the scattering operator $\Lambda_\kappa : L^2(\partial \mathcal{B}_t)^3 \rightarrow L^2(\partial \mathcal{B}_t)^3$ by

$$\Lambda_\kappa(\boldsymbol{\tau}) = \mathbf{v}^\kappa|_{\partial \mathcal{B}_t}, \quad \kappa = \circ, 1, 2, \dots, \quad (11)$$

where \mathbf{v}^κ solves (5). Then, there exists the factorization

$$\Lambda_\kappa = \mathcal{S}_\kappa^* T_\kappa \mathcal{S}_\kappa \quad (12)$$

such that $\mathcal{S}_\kappa : L^2(\partial \mathcal{B}_t)^3 \rightarrow S(\mathcal{D}_\kappa^* \cup \Gamma_\kappa \cup \partial \mathcal{D}_\kappa^o)$ is defined by

$$\mathcal{S}_\kappa(\boldsymbol{\tau}) := (\mathbf{u}^f|_{\mathcal{D}_\kappa^* \setminus \overline{\Gamma_\kappa}}, \nabla \mathbf{u}^f|_{\mathcal{D}_\kappa^* \setminus \overline{\Gamma_\kappa}}, \mathbf{t}[\mathbf{u}^f]|_{\Gamma_\kappa}, \mathbf{t}[\mathbf{u}^f]|_{\partial \mathcal{D}_\kappa^o}), \quad (13)$$

whose adjoint operator $\mathcal{S}_\kappa^* : \tilde{S}(\mathcal{D}_\kappa^* \cup \Gamma_\kappa \cup \partial\mathcal{D}_\kappa^o) \rightarrow L^2(\partial\mathcal{B}_t)^3$ takes the form

$$\mathcal{S}_\kappa^*(\Phi, \mathbf{\Phi}, \varphi, \phi) := \mathbf{v}^*(\xi), \quad \xi \in \partial\mathcal{B}_t, \quad (14)$$

where $\mathbf{v}^* \in H^1(\mathcal{B} \setminus \overline{\Gamma_\kappa \cup \partial\mathcal{D}_\kappa^o})^3$ solves

$$\begin{aligned} \nabla \cdot \mathbf{C} : \nabla \mathbf{v}^*(\xi) + \rho\omega^2 \mathbf{v}^*(\xi) + \mathbf{1}(\mathcal{D}_\kappa^* \setminus \overline{\Gamma_\kappa})(\Phi - \nabla \cdot \mathbf{\Phi}) &= \mathbf{0}, & \xi \in \mathcal{B} \setminus \overline{\Gamma_\kappa \cup \partial\mathcal{D}_\kappa^o}, \\ \llbracket \mathbf{t}[\mathbf{v}^*] \rrbracket(\xi) = -\mathbf{n} \cdot \mathbf{\Phi}(\xi), \quad \llbracket \mathbf{v}^* \rrbracket(\xi) &= \mathbf{0}, & \xi \in \partial\mathcal{D}_\kappa^* \setminus \overline{\Gamma_\kappa}, \\ \llbracket \mathbf{v}^* \rrbracket(\xi) = \varphi, \quad \llbracket \mathbf{t}[\mathbf{v}^*] - \mathbf{1}(\mathcal{D}_\kappa^* \cap \Gamma_\kappa) \mathbf{n} \cdot \mathbf{\Phi} \rrbracket(\xi) &= -\mathbf{1}(\partial\mathcal{D}_\kappa^* \cap \Gamma_\kappa) \mathbf{n} \cdot \mathbf{\Phi}(\xi), & \xi \in \Gamma_\kappa, \\ \llbracket \mathbf{v}^* \rrbracket(\xi) = \phi, \quad \llbracket \mathbf{t}[\mathbf{v}^*] \rrbracket(\xi) &= \mathbf{0}, & \xi \in \partial\mathcal{D}_\kappa^o, \\ \mathbf{t}[\mathbf{v}^*](\xi) &= \mathbf{0}, & \xi \in \partial\mathcal{B}_t, \end{aligned} \quad (15)$$

wherein $\mathbf{t}[\mathbf{v}^*] := \mathbf{n} \cdot \mathbf{C} : \nabla \mathbf{v}^*$. This may be observed by (i) premultiplying the first of (15) by $\bar{\mathbf{u}}^f$, and (ii) postmultiplying the conjugated first of (3) by \mathbf{v}^* . Integration by parts over $\mathcal{B} \setminus \overline{\Gamma_\kappa \cup \partial\mathcal{D}_\kappa^o}$ followed by application of the contact condition over $\Gamma_\kappa \cup \partial\mathcal{D}_\kappa^o$ and summation of the results yield

$$\int_{\partial\mathcal{B}_t} \bar{\boldsymbol{\tau}} \cdot \mathbf{v}^* dS_\xi = \int_{\mathcal{D}_\kappa^* \setminus \overline{\Gamma_\kappa}} (\bar{\mathbf{u}}^f \cdot \Phi + \nabla \bar{\mathbf{u}}^f : \mathbf{\Phi}) dV_\xi + \int_{\Gamma_\kappa} \bar{\mathbf{t}}[\mathbf{u}^f] \cdot \varphi dS_\xi + \int_{\partial\mathcal{D}_\kappa^o} \bar{\mathbf{t}}[\mathbf{u}^f] \cdot \phi dS_\xi,$$

which substantiates (14) via $\langle (\Phi, \mathbf{\Phi}, \varphi, \phi), \mathcal{S}_\kappa(\boldsymbol{\tau}) \rangle_{\mathcal{D}_\kappa^* \cup \Gamma_\kappa \cup \partial\mathcal{D}_\kappa^o} = \langle \mathbf{v}^*, \boldsymbol{\tau} \rangle_{\partial\mathcal{B}_t}$. Here,

$$\begin{aligned} \langle \cdot, \cdot \rangle_{\mathcal{D}_\kappa^* \cup \Gamma_\kappa \cup \partial\mathcal{D}_\kappa^o} &:= \langle \tilde{S}(\mathcal{D}_\kappa^* \cup \Gamma_\kappa \cup \partial\mathcal{D}_\kappa^o), S(\mathcal{D}_\kappa^* \cup \Gamma_\kappa \cup \partial\mathcal{D}_\kappa^o) \rangle, \\ \langle \cdot, \cdot \rangle_{\partial\mathcal{B}_t} &:= \langle \tilde{H}^{\frac{1}{2}}(\partial\mathcal{B}_t)^3, H^{-\frac{1}{2}}(\partial\mathcal{B}_t)^3 \rangle, \end{aligned} \quad (16)$$

extend L^2 inner products. In this setting, the middle operator $T_\kappa : S(\mathcal{D}_\kappa^* \cup \Gamma_\kappa \cup \partial\mathcal{D}_\kappa^o) \rightarrow \tilde{S}(\mathcal{D}_\kappa^* \cup \Gamma_\kappa \cup \partial\mathcal{D}_\kappa^o)$ is given by

$$\begin{aligned} T_\kappa(\mathbf{u}^f|_{\mathcal{D}_\kappa^* \setminus \overline{\Gamma_\kappa}}, \nabla \mathbf{u}^f|_{\mathcal{D}_\kappa^* \setminus \overline{\Gamma_\kappa}}, \mathbf{t}[\mathbf{u}^f]|_{\Gamma_\kappa}, \mathbf{t}[\mathbf{u}^f]|_{\partial\mathcal{D}_\kappa^o}) &:= \\ ((\rho_\kappa - \rho)\omega^2 \mathbf{w}^\kappa|_{\mathcal{D}_\kappa^* \setminus \overline{\Gamma_\kappa}}, -(\mathbf{C}_\kappa - \mathbf{C}) : \nabla \mathbf{w}^\kappa|_{\mathcal{D}_\kappa^* \setminus \overline{\Gamma_\kappa}}, \llbracket \mathbf{u} \rrbracket|_{\Gamma_\kappa}, \mathbf{u}^\kappa|_{\partial\mathcal{D}_\kappa^o}). \end{aligned} \quad (17)$$

4 Properties of operators

Assumption 4.1. *Given $\kappa \in \{0, 1, \dots\}$ and $j \in \{0, 1, \dots, N_\kappa^o\}$, suppose that (a) \mathcal{D}_κ^o may be decomposed into simply-connected components $\mathcal{D}_{\kappa,j}^o \subset \mathcal{D}_\kappa^o$, and (b) Γ_κ consists of $M_\kappa \geq 1$ (possibly disjoint) analytic surfaces $S_m \subset \Gamma_\kappa$, $m = 1, \dots, M_\kappa$, with the unique continuation $\partial\mathbf{D}_m$ identifying the “interior” domain $\mathbf{D}_m \subset \mathcal{B}$. Then for any j (resp. m), it is assumed that $\omega > 0$ is not a “Neumann” eigenfrequency of the Navier equation in $\mathcal{D}_{\kappa,j}^o$ (resp. \mathbf{D}_m), i.e., as long as $\mathbf{u}_j \in H^1(\mathcal{D}_{\kappa,j}^o)^3$ and $\mathbf{u}_m \in H^1(\mathbf{D}_m)^3$ satisfying*

$$\begin{cases} \nabla \cdot (\mathbf{C} : \nabla \mathbf{u}_j) + \rho\omega^2 \mathbf{u}_j = \mathbf{0} & \text{in } \mathcal{D}_{\kappa,j}^o \\ \mathbf{n} \cdot \mathbf{C} : \nabla \mathbf{u}_j = \mathbf{0} & \text{on } \partial\mathcal{D}_{\kappa,j}^o \end{cases} \wedge \begin{cases} \nabla \cdot (\mathbf{C}_\kappa : \nabla \mathbf{u}_m) + \rho_\kappa \omega^2 \mathbf{u}_m = \mathbf{0} & \text{in } \mathbf{D}_m \\ \mathbf{n} \cdot \mathbf{C}_\kappa : \nabla \mathbf{u}_m = \mathbf{0} & \text{on } \partial\mathbf{D}_m \end{cases}, \quad (18)$$

vanish identically in $\mathcal{D}_{\kappa,j}^o$ and \mathbf{D}_m respectively. If \mathbf{D}_m is bounded, the real eigenfrequencies of (18) form a discrete set [12, 13].

Lemma 4.1. *In light of the unique continuation principle, the operator $\mathcal{S}_\kappa: L^2(\partial\mathcal{B}_t)^3 \rightarrow S(\mathcal{D}_\kappa^* \cup \Gamma_\kappa \cup \partial\mathcal{D}_\kappa^o)$ is injective at all t_κ .*

Lemma 4.2. *Let*

$$H_\Delta = \{ \hat{\mathbf{u}} \in H^1(\mathcal{D}_\kappa^*)^3 \mid \nabla \cdot \mathbf{C} : \nabla \hat{\mathbf{u}} + \rho\omega^2 \hat{\mathbf{u}} = \mathbf{0} \text{ in } \mathcal{D}_\kappa^* \},$$

and define the map $(\hat{S}_1, \hat{S}_2, \hat{S}_3): H_\Delta \rightarrow L^2(\mathcal{D}_\kappa^* \setminus \overline{\Gamma_\kappa})^3 \times L^2(\mathcal{D}_\kappa^* \setminus \overline{\Gamma_\kappa})^{3 \times 3} \times L^2(\Gamma_\kappa \cap \overline{\mathcal{D}_\kappa^*})^3$ such that

$$(\hat{S}_1, \hat{S}_2, \hat{S}_3)(\hat{\mathbf{u}}) = (\hat{\mathbf{u}}|_{\mathcal{D}_\kappa^* \setminus \overline{\Gamma_\kappa}}, \nabla \hat{\mathbf{u}}|_{\mathcal{D}_\kappa^* \setminus \overline{\Gamma_\kappa}}, \mathbf{t}[\hat{\mathbf{u}}]|_{\Gamma_\kappa \cap \overline{\mathcal{D}_\kappa^*}}), \quad \mathbf{t}[\hat{\mathbf{u}}] = \mathbf{n} \cdot \mathbf{C} : \nabla \hat{\mathbf{u}},$$

then $\mathfrak{S}(H_\Delta) := \hat{S}_1(H_\Delta) \times \hat{S}_2(H_\Delta) \times (\hat{S}_3(H_\Delta) \oplus H^{-1/2}(\Gamma_\kappa \setminus \overline{\mathcal{D}_\kappa^*})^3) \times H^{-1/2}(\partial\mathcal{D}_\kappa^o)^3 = \overline{\mathcal{R}(\mathcal{S}_\kappa)}$ where the latter denotes the closure of the range of \mathcal{S}_κ .

Proof. Observe that the restriction of $\mathbf{u}^f \in H^1(\mathcal{B})^3$, satisfying (3), to \mathcal{D}_κ^* belongs to H_Δ , hence $\mathcal{R}(\mathcal{S}_\kappa) \subset \mathfrak{S}(H_\Delta)$. To prove the claim, it is then sufficient to establish that $\mathcal{S}_\kappa^*: \mathfrak{S}(H_\Delta) \rightarrow L^2(\partial\mathcal{B}_t)^3$ given by

$$\begin{aligned} \frac{1}{2} \mathcal{S}_\kappa^*(\Phi, \mathbf{F}, \varphi \oplus \psi, \phi) &= \int_{\mathcal{D}_\kappa^* \setminus \overline{\Gamma_\kappa}} [\Phi(\mathbf{y}) \cdot \mathbf{G}(\boldsymbol{\xi}, \mathbf{y}) + \mathbf{F}(\mathbf{y}) : \nabla \mathbf{G}(\boldsymbol{\xi}, \mathbf{y})] dV_{\mathbf{y}} + \\ &\int_{\Gamma_\kappa \cap \overline{\mathcal{D}_\kappa^*}} \varphi(\mathbf{y}) \cdot \mathbf{T}(\boldsymbol{\xi}, \mathbf{y}) dS_{\mathbf{y}} + \int_{\Gamma_\kappa \setminus \overline{\mathcal{D}_\kappa^*}} \psi(\mathbf{y}) \cdot \mathbf{T}(\boldsymbol{\xi}, \mathbf{y}) dS_{\mathbf{y}} + \int_{\partial\mathcal{D}_\kappa^o} \phi(\mathbf{y}) \cdot \mathbf{T}(\boldsymbol{\xi}, \mathbf{y}) dS_{\mathbf{y}}, \end{aligned} \quad (19)$$

is injective on $\mathfrak{S}(H_\Delta)$. Suppose that there exists $(\Phi, \mathbf{F}, \varphi \oplus \psi, \phi) = (\mathbf{u}^i, \nabla \mathbf{u}^i, \mathbf{t}[\mathbf{u}^i] \oplus \psi, \phi)$ – with $\mathbf{u}^i \in H^1(\mathcal{D}_\kappa^*)^3$ satisfying $\nabla \cdot \mathbf{C} : \nabla \mathbf{u}^i + \rho\omega^2 \mathbf{u}^i = \mathbf{0}$ in \mathcal{D}_κ^* while $(\psi, \phi) \in \tilde{H}^{1/2}(\Gamma_\kappa \setminus \overline{\mathcal{D}_\kappa^*})^3 \times \tilde{H}^{1/2}(\partial\mathcal{D}_\kappa^o)^3$ – such that $\mathcal{S}_\kappa^*(\mathbf{u}^i, \nabla \mathbf{u}^i, \mathbf{t}[\mathbf{u}^i] \oplus \psi, \phi) = \mathbf{0}$. Since by construction $\mathbf{v}^\kappa(\boldsymbol{\xi}) = \mathcal{S}_\kappa^*(\cdot)$ on $\boldsymbol{\xi} \in \partial\mathcal{B}_t$, it is evident from (5) that \mathbf{v}^κ has trivial Dirichlet and Neumann traces on $\partial\mathcal{B}_t$, and thus, the unique continuation principle reads $\mathbf{v}^\kappa = \mathbf{0}$ in $\mathcal{B} \setminus \overline{\Gamma_\kappa \cup \mathcal{D}_\kappa^*}$. From (a) properties of the layer potentials i.e., $\phi = \mathbf{u}^\kappa$ and $\psi = \llbracket \mathbf{v}^\kappa \rrbracket$, (b) fifth of (5) which reads $\mathbf{t}^f = \mathbf{0}$ on $\partial\mathcal{D}_\kappa^o$, and (c) Assumption 4.1 indicating that $\omega > 0$ is not a Neumann eigenfrequency of the Navier equation affiliated with any simply-connected subset of \mathcal{D}_κ^o , one may conclude that $\psi = \phi = \mathbf{0}$. Now, on denoting $\Gamma_\kappa^l = \Gamma_\kappa \cap \overline{\mathcal{D}_\kappa^*}$ and $\mathcal{B}^* = \mathcal{B} \setminus \overline{\Gamma_\kappa^l \cup \partial\mathcal{D}_\kappa^*}$, let $\forall \boldsymbol{\xi} \in \mathcal{B} \setminus \overline{\Gamma_\kappa^l}$,

$$\mathbf{v}(\boldsymbol{\xi}) = \int_{\mathcal{D}_\kappa^* \setminus \overline{\Gamma_\kappa}} [\mathbf{u}^i(\mathbf{y}) \cdot \mathbf{G}(\boldsymbol{\xi}, \mathbf{y}) + \nabla \mathbf{u}^i(\mathbf{y}) : \nabla \mathbf{G}(\boldsymbol{\xi}, \mathbf{y})] dV_{\mathbf{y}} + \int_{\Gamma_\kappa^l} \mathbf{t}[\mathbf{u}^i](\mathbf{y}) \cdot \mathbf{T}(\boldsymbol{\xi}, \mathbf{y}) dS_{\mathbf{y}}. \quad (20)$$

From the regularity of volume potentials, one may infer that $\forall \mathbf{v}' \in H^1(\mathcal{B}^*)$, $\mathbf{v} \in H^1(\mathcal{B}^*)$ satisfies

$$\begin{aligned} \int_{\mathcal{B}^*} [\rho\omega^2 \mathbf{v}' \cdot \mathbf{v} - \nabla \mathbf{v}' : \mathbf{C} : \nabla \mathbf{v}] dV_{\boldsymbol{\xi}} - \int_{\Gamma_\kappa^l} \llbracket \mathbf{v}' \rrbracket \cdot (\mathbf{n} \cdot [\mathbf{C} : \nabla \mathbf{v} - \nabla \mathbf{u}^i]) dS_{\boldsymbol{\xi}} = \\ - \int_{\mathcal{D}_\kappa^* \setminus \overline{\Gamma_\kappa}} [\mathbf{v}' \cdot \mathbf{u}^i + \nabla \mathbf{v}' : \nabla \mathbf{u}^i] dV_{\boldsymbol{\xi}}. \end{aligned} \quad (21)$$

Note that $\mathbf{v} = \mathcal{S}_\kappa^*(\mathbf{u}^i, \nabla \mathbf{u}^i, \mathbf{t}[\mathbf{u}^i] \oplus \mathbf{0}, \mathbf{0})$ on $\partial\mathcal{B}_t$, then $\mathcal{S}_\kappa^*(\cdot) = \mathbf{0}$ implies that $\mathbf{v} = \mathbf{0}$ in $\mathcal{B}^* \setminus \overline{\mathcal{D}_\kappa^*}$. Then by setting $\mathbf{v}' = \bar{\mathbf{u}}^i$, (21) may be recast as

$$\int_{\mathcal{D}_\kappa^* \setminus \overline{\Gamma_\kappa}} [\rho\omega^2 \bar{\mathbf{u}}^i \cdot \mathbf{v} - \nabla \bar{\mathbf{u}}^i : \mathbf{C} : \nabla \mathbf{v}] dV_{\boldsymbol{\xi}} = - \|\mathbf{u}^i\|_{H^1(\mathcal{D}_\kappa^* \setminus \overline{\Gamma_\kappa})^3}^2. \quad (22)$$

Also, on recalling $\nabla \cdot \mathbf{C} : \nabla \mathbf{u}^i + \rho \omega^2 \mathbf{u}^i = \mathbf{0}$ in \mathcal{D}_κ^* , it follows that

$$\int_{\mathcal{D}_\kappa^* \setminus \overline{\Gamma_\kappa}} [\rho \omega^2 \bar{\mathbf{u}}^i \cdot \mathbf{v} - \nabla \bar{\mathbf{u}}^i : \mathbf{C} : \nabla \mathbf{v}] dV_\xi = \|\mathbf{t}[\mathbf{u}^i]\|_{L^2(\Gamma_\kappa^i)}^2. \quad (23)$$

Combining (22) and (23) reads $(\boldsymbol{\Phi}, \Phi, \boldsymbol{\varphi}) = \mathbf{0}$ which completes the proof. \square

Lemma 4.3. *Under Assumption 2.2, the operator $\mathcal{S}_\kappa^* : \tilde{S}(\mathcal{D}_\kappa^* \cup \Gamma_\kappa \cup \partial \mathcal{D}_\kappa^o) \rightarrow L^2(\partial \mathcal{B}_t)^3$ is compact and has a dense range.*

Proof. The compactness of \mathcal{S}_κ^* is established by the smooth kernels in its integral form (19), and its dense range results from the injectivity of \mathcal{S}_κ per Lemma 4.1. \square

Assumption 4.2. *Under Assumptions 2.1-2.3, given $(\mathbf{f}^\kappa, \mathbf{g}^\kappa) \in H^{-1/2}(\partial \mathcal{D}_\kappa^*)^3 \times H^{1/2}(\partial \mathcal{D}_\kappa^*)^3$, consider the solution $(\mathbf{u}^\kappa, \mathbf{w}^\kappa) \in H^1(\mathcal{D}_\kappa^*)^3 \times H^1(\mathcal{D}_\kappa^* \setminus \overline{\Gamma_\kappa})^3$ to the interior transmission problem (ITP)*

$$\begin{cases} \text{ITP}(\mathcal{D}_\kappa^*, \Gamma_\kappa; \{\mathbf{C}, \rho\}, \{\mathbf{C}_\kappa, \rho_\kappa\}, \mathbf{K}_\kappa; \mathbf{f}^\kappa, \mathbf{g}^\kappa): \\ \left\{ \begin{array}{ll} \nabla \cdot [\mathbf{C}_\kappa(\boldsymbol{\xi}) : \nabla \mathbf{w}^\kappa](\boldsymbol{\xi}) + \rho_\kappa(\boldsymbol{\xi}) \omega^2 \mathbf{w}^\kappa(\boldsymbol{\xi}) = \mathbf{0}, & \boldsymbol{\xi} \in \mathcal{D}_\kappa^* \setminus \overline{\Gamma_\kappa}, \\ \nabla \cdot \mathbf{C} : \nabla \mathbf{u}^\kappa(\boldsymbol{\xi}) + \rho \omega^2 \mathbf{u}^\kappa(\boldsymbol{\xi}) = \mathbf{0}, & \boldsymbol{\xi} \in \mathcal{D}_\kappa^*, \\ \mathbf{t}[\mathbf{w}^\kappa](\boldsymbol{\xi}) - \mathbf{t}[\mathbf{u}^\kappa](\boldsymbol{\xi}) = \mathbf{f}^\kappa(\boldsymbol{\xi}), \quad [\mathbf{w}^\kappa - \mathbf{u}^\kappa](\boldsymbol{\xi}) = \mathbf{g}^\kappa(\boldsymbol{\xi}), & \boldsymbol{\xi} \in \partial \mathcal{D}_\kappa^* \setminus \overline{\Gamma_\kappa}, \\ \mathbf{t}[\mathbf{w}^\kappa](\boldsymbol{\xi}) = \mathbf{K}_\kappa(\boldsymbol{\xi}) \llbracket \mathbf{w}^\kappa \rrbracket(\boldsymbol{\xi}), \quad \llbracket \mathbf{t}[\mathbf{w}^\kappa] \rrbracket(\boldsymbol{\xi}) = \mathbf{0}, & \boldsymbol{\xi} \in \Gamma_\kappa \cap \mathcal{D}_\kappa^*, \\ \mathbf{t}[\mathbf{w}^\kappa](\boldsymbol{\xi}) - \mathbf{t}[\mathbf{u}^\kappa](\boldsymbol{\xi}) = \mathbf{f}^\kappa(\boldsymbol{\xi}), \quad \mathbf{t}[\mathbf{w}^\kappa](\boldsymbol{\xi}) = \mathbf{K}_\kappa(\boldsymbol{\xi})[\mathbf{g}^\kappa + \mathbf{u}^\kappa - \mathbf{w}^\kappa](\boldsymbol{\xi}), & \boldsymbol{\xi} \in \Gamma_\kappa \cap \partial \mathcal{D}_\kappa^*, \end{array} \right. \end{cases} \quad (24)$$

wherein

$$\mathbf{t}[\mathbf{u}^\kappa](\boldsymbol{\xi}) = \mathbf{n}(\boldsymbol{\xi}) \cdot \mathbf{C} : \nabla \mathbf{u}^\kappa(\boldsymbol{\xi}), \quad \mathbf{t}[\mathbf{w}^\kappa](\boldsymbol{\xi}) = \mathbf{n}(\boldsymbol{\xi}) \cdot \mathbf{C}_\kappa(\boldsymbol{\xi}) : \nabla \mathbf{w}^\kappa(\boldsymbol{\xi}), \quad \boldsymbol{\xi} \in \Gamma_\kappa \cup \partial \mathcal{D}_\kappa^*.$$

It is assumed that $\forall t_\kappa, \omega$ is such that (24) remains wellposed i.e., for $(\mathbf{f}^\kappa, \mathbf{g}^\kappa) = \mathbf{0}$, the ITP does not admit a nontrivial solution $(\mathbf{u}^\kappa, \mathbf{w}^\kappa)$. For $\Gamma_\kappa = \emptyset$, the elastodynamics ITP, with varying restrictions on \mathbf{C} and $\mathbf{C}_\kappa(\boldsymbol{\xi})$, is analyzed by [22, 13, 12, 20] following the variational method introduced by [35]. In the most general case, under Assumptions 2.2 and 2.3, (24) with $\Gamma_\kappa = \emptyset$ is well-posed when ω does not belong to (at most) a countable set of transmission eigenvalues [13]. The latter is also concluded in a recent study of acoustic ITP for penetrable obstacles with sound-hard cracks [5]. Similar analysis could be applied to (24) which is beyond the scope of the present study.

Lemma 4.4. *Operator $T_\kappa : \mathfrak{S}(H_\Delta) \rightarrow \tilde{S}(\mathcal{D}_\kappa^* \cup \Gamma_\kappa \cup \partial \mathcal{D}_\kappa^o)$ in (17) is bounded and satisfies*

$$\Im \langle T_\kappa \boldsymbol{\Xi}, \boldsymbol{\Xi} \rangle_{\mathcal{D}_\kappa^* \cup \Gamma_\kappa \cup \partial \mathcal{D}_\kappa^o} > 0, \quad (25)$$

$\forall \boldsymbol{\Xi} \in \mathfrak{S}(H_\Delta) : \boldsymbol{\Xi} \neq \mathbf{0}$. Consequently, T_κ is also injective provided that ω is not a transmission eigenvalue of (24) per Assumption 4.2.

Proof. The well-posedness of (5) establish the boundedness of T_κ . Now, consider \mathbf{v}^κ satisfying (61) with $(\mathbf{u}^f|_{\mathcal{D}_\kappa^* \setminus \overline{\Gamma_\kappa}}, \nabla \mathbf{u}^f|_{\mathcal{D}_\kappa^* \setminus \overline{\Gamma_\kappa}}, \mathbf{t}[\mathbf{u}^f]|_{\Gamma_\kappa}, \mathbf{t}[\mathbf{u}^f]|_{\partial \mathcal{D}_\kappa^o}) = \Xi$. Taking $\mathbf{v}' = \mathbf{v}^\kappa$ in \mathcal{B}_κ^- and $\mathbf{v}' = \mathbf{w}^\kappa - \mathbf{u}^f$ in $\mathcal{D}_\kappa^* \setminus \overline{\Gamma_\kappa}$, observe from (61) that

$$\Im \langle T_\kappa \Xi, \Xi \rangle_{\mathcal{D}_\kappa^* \cup \Gamma_\kappa \cup \partial \mathcal{D}_\kappa^o} = -\Im \left(\int_{\mathcal{D}_\kappa^* \setminus \overline{\Gamma_\kappa}} \nabla \bar{\mathbf{w}}^\kappa : \mathbf{C}_\kappa : \nabla \mathbf{w}^\kappa \, dV_\xi + \int_{\Gamma_\kappa} \llbracket \bar{\mathbf{v}}^\kappa \rrbracket \cdot \mathbf{K}_\kappa \llbracket \mathbf{v}^\kappa \rrbracket \, dS_\xi \right), \quad (26)$$

whereby (25) follows immediately from Assumption 2.2. Now, let $T_\kappa \Xi = \mathbf{0}$, then (26), second of (4), the unique continuation principle, and (9) imply that $\mathcal{S}_\kappa^* T_\kappa \Xi = \mathbf{0}$. Then, Lemma 4.5 reads $\Xi = \mathbf{0}$ which proves the injectivity of T_κ . \square

Lemma 4.5. *Under Assumption 4.2, the operator $\mathcal{V}_\kappa = \mathcal{S}_\kappa^* T_\kappa : \mathfrak{S}(H_\Delta) \rightarrow L^2(\partial \mathcal{B}_t)^3$ is compact and injective with dense range.*

Proof. Compactness of \mathcal{V}_κ follows immediately from Lemmas 4.3 and 4.4 which respectively establish the compactness of \mathcal{S}_κ^* and the boundedness of T_κ . To demonstrate the injectivity of \mathcal{V}_κ , let

$$(\hat{\mathbf{u}}|_{\mathcal{D}_\kappa^* \setminus \overline{\Gamma_\kappa}}, \nabla \hat{\mathbf{u}}|_{\mathcal{D}_\kappa^* \setminus \overline{\Gamma_\kappa}}, \mathbf{t}[\hat{\mathbf{u}}]|_{\Gamma_\kappa \cap \overline{\mathcal{D}_\kappa^*}} \oplus \boldsymbol{\psi}, \boldsymbol{\phi}) \in \mathfrak{S}(H_\Delta), \quad (\boldsymbol{\psi}, \boldsymbol{\phi}) \in H^{-1/2}(\Gamma_\kappa \setminus \overline{\mathcal{D}_\kappa^*})^3 \times H^{-1/2}(\partial \mathcal{D}_\kappa^o)^3,$$

such that $\mathcal{V}_\kappa(\hat{\mathbf{u}}|_{\mathcal{D}_\kappa^* \setminus \overline{\Gamma_\kappa}}, \nabla \hat{\mathbf{u}}|_{\mathcal{D}_\kappa^* \setminus \overline{\Gamma_\kappa}}, \mathbf{t}[\hat{\mathbf{u}}]|_{\Gamma_\kappa \cap \overline{\mathcal{D}_\kappa^*}} \oplus \boldsymbol{\psi}, \boldsymbol{\phi}) = \mathbf{0}$. Since by definition $\mathbf{v}^\kappa = \mathcal{V}_\kappa(\cdot)$ on $\partial \mathcal{B}_t$, one may observe that \mathbf{v}^κ satisfying (5) has trivial Dirichlet and Neumann traces on $\partial \mathcal{B}_t$ so that by the unique continuation principle $\mathbf{v}^\kappa = \mathbf{0}$ in \mathcal{B}_κ^- . Now, from (a) second and fifth of (5), and (b) Assumption 4.1 indicating that $\omega > 0$ is not a Neumann eigenfrequency of the Navier equation affiliated with any simply-connected subset of \mathcal{D}_κ^o , one may conclude that $\boldsymbol{\psi} = \boldsymbol{\phi} = \mathbf{0}$. Next, let us define \mathbf{w}^κ such that $\mathbf{w}^\kappa = \hat{\mathbf{u}} + \mathbf{v}^\kappa$ in \mathcal{D}_κ^* , then the pair $(\hat{\mathbf{u}}, \mathbf{w}^\kappa)$ satisfies the interior transmission problem (24) with trivial boundary potentials i.e., $(\mathbf{f}^\kappa, \mathbf{g}^\kappa) = \mathbf{0}$. Since ω is not a transmission eigenvalue as per Assumption 4.2, one may deduce that $\hat{\mathbf{u}} = \mathbf{0}$ in $\mathcal{D}_\kappa^* \setminus \overline{\Gamma_\kappa}$. Subsequently, $\nabla \hat{\mathbf{u}} = \mathbf{0}$ in $\mathcal{D}_\kappa^* \setminus \overline{\Gamma_\kappa}$, and $\mathbf{t}[\hat{\mathbf{u}}] = \mathbf{0}$ on $\Gamma_\kappa \cap \overline{\mathcal{D}_\kappa^*}$ which proves the injectivity of \mathcal{V}_κ .

Denseness of the range of \mathcal{V}_κ may be established by showing that the adjoint operator \mathcal{V}_κ^* is injective. In this vein, from definition, $\mathcal{V}_\kappa^* : L^2(\partial \mathcal{B}_t)^3 \rightarrow \tilde{S}(\mathcal{D}_\kappa^* \cup \Gamma_\kappa \cup \partial \mathcal{D}_\kappa^o)$ is given by

$$\mathcal{V}_\kappa^*(\boldsymbol{\tau}) = ((\rho_\kappa - \rho)\omega^2 \mathbf{u}^\tau|_{\mathcal{D}_\kappa^* \setminus \overline{\Gamma_\kappa}}, -(\overline{\mathbf{C}_\kappa} - \mathbf{C}) : \nabla \mathbf{u}^\tau|_{\mathcal{D}_\kappa^* \setminus \overline{\Gamma_\kappa}}, \llbracket \mathbf{u}^\tau \rrbracket|_{\Gamma_\kappa}, \mathbf{u}^\tau|_{\partial \mathcal{D}_\kappa^o}), \quad (27)$$

where $\mathbf{u}^\tau \in H^1(\mathcal{B}_\kappa^- \cup \mathcal{D}_\kappa^* \setminus \overline{\Gamma_\kappa})^3$ solves

$$\begin{aligned} \nabla \cdot \mathbf{C} : \nabla \mathbf{u}^\tau(\boldsymbol{\xi}) + \rho \omega^2 \mathbf{u}^\tau(\boldsymbol{\xi}) + \mathbf{1}(\mathcal{D}_\kappa^* \setminus \overline{\Gamma_\kappa})[\mathbf{f}^\tau + \nabla \cdot \boldsymbol{\sigma}^\tau](\boldsymbol{\xi}) &= \mathbf{0}, & \boldsymbol{\xi} \in \mathcal{B}_\kappa^- \cup \mathcal{D}_\kappa^* \setminus \overline{\Gamma_\kappa}, \\ \mathbf{t}[\mathbf{u}^\tau](\boldsymbol{\xi}) + \mathbf{1}(\overline{\mathcal{D}_\kappa^*} \cap \Gamma_\kappa) \mathbf{n} \cdot \boldsymbol{\sigma}^\tau(\boldsymbol{\xi}) &= \overline{\mathbf{K}_\kappa}(\boldsymbol{\xi}) \llbracket \mathbf{u}^\tau \rrbracket(\boldsymbol{\xi}), & \boldsymbol{\xi} \in \Gamma_\kappa, \\ \llbracket \mathbf{t}[\mathbf{u}^\tau] + \mathbf{1}(\mathcal{D}_\kappa^* \cap \Gamma_\kappa) \mathbf{n} \cdot \boldsymbol{\sigma}^\tau(\boldsymbol{\xi}) \rrbracket(\boldsymbol{\xi}) &= \mathbf{1}(\partial \mathcal{D}_\kappa^* \cap \Gamma_\kappa) \mathbf{n} \cdot \boldsymbol{\sigma}^\tau(\boldsymbol{\xi}), & \boldsymbol{\xi} \in \Gamma_\kappa, \\ \llbracket \mathbf{t}[\mathbf{u}^\tau] \rrbracket(\boldsymbol{\xi}) &= \mathbf{n} \cdot \boldsymbol{\sigma}^\tau(\boldsymbol{\xi}), \quad \llbracket \mathbf{u}^\tau \rrbracket(\boldsymbol{\xi}) = \mathbf{0}, & \boldsymbol{\xi} \in \partial \mathcal{D}_\kappa^* \setminus \overline{\Gamma_\kappa}, \\ \mathbf{t}[\mathbf{u}^\tau](\boldsymbol{\xi}) &= \mathbf{0}, & \boldsymbol{\xi} \in \partial \mathcal{D}_\kappa^o, \\ \mathbf{t}[\mathbf{u}^\tau](\boldsymbol{\xi}) &= \boldsymbol{\tau}, & \boldsymbol{\xi} \in \partial \mathcal{B}_t. \end{aligned} \quad (28)$$

where $\mathbf{t}[\mathbf{u}^\tau] := \mathbf{n} \cdot \mathbf{C} : \nabla \mathbf{u}^\tau$, and

$$\mathbf{f}^\tau(\boldsymbol{\xi}) := (\rho_\kappa(\boldsymbol{\xi}) - \rho)\omega^2 \mathbf{u}^\tau(\boldsymbol{\xi}), \quad \boldsymbol{\sigma}^\tau(\boldsymbol{\xi}) := (\overline{\mathbf{C}_\kappa}(\boldsymbol{\xi}) - \mathbf{C}) : \nabla \mathbf{u}^\tau(\boldsymbol{\xi}), \quad \boldsymbol{\xi} \in \mathcal{D}_\kappa^* \setminus \overline{\Gamma_\kappa}.$$

This may be observed by (i) premultiplying the first of (5) by $\overline{\mathbf{u}^\tau}$, and (ii) postmultiplying the conjugated first of (28) by \mathbf{v}^κ . Integration by parts over $\mathcal{B}_\kappa^- \cup \mathcal{D}_\kappa^* \setminus \overline{\Gamma_\kappa}$ followed by application of the contact condition over $\Gamma_\kappa \cup \partial \mathcal{D}_\kappa$ and summation of the results yield

$$\begin{aligned} \langle \overline{\mathbf{v}^\kappa}, \boldsymbol{\tau} \rangle_{\partial \mathcal{B}_t} &= \langle ((\rho_\kappa - \rho)\omega^2 \mathbf{u}^\tau|_{\mathcal{D}_\kappa^* \setminus \overline{\Gamma_\kappa}}, -(\overline{\mathbf{C}_\kappa} - \mathbf{C}) : \nabla \mathbf{u}^\tau|_{\mathcal{D}_\kappa^* \setminus \overline{\Gamma_\kappa}}, \llbracket \mathbf{u}^\tau \rrbracket|_{\Gamma_\kappa}, \mathbf{u}^\tau|_{\partial \mathcal{D}_\kappa^o}), \\ &\quad (\mathbf{u}^f|_{\mathcal{D}_\kappa^* \setminus \overline{\Gamma_\kappa}}, \nabla \mathbf{u}^f|_{\mathcal{D}_\kappa^* \setminus \overline{\Gamma_\kappa}}, \mathbf{t}[\mathbf{u}^f]|_{\Gamma_\kappa}, \mathbf{t}[\mathbf{u}^f]|_{\partial \mathcal{D}_\kappa^o}) \rangle_{\mathcal{D}_\kappa^* \cup \Gamma_\kappa \cup \partial \mathcal{D}_\kappa^o}, \end{aligned}$$

substantiating (28) as the adjoint operator. Next, let $\boldsymbol{\tau} \in L^2(\partial \mathcal{B}_t)^3$ and assume that $\mathcal{V}_\kappa^*(\boldsymbol{\tau}) = \mathbf{0}$, i.e.,

$$(\mathbf{u}^\tau|_{\mathcal{D}_\kappa^* \setminus \overline{\Gamma_\kappa}}, \nabla \mathbf{u}^\tau|_{\mathcal{D}_\kappa^* \setminus \overline{\Gamma_\kappa}}, \llbracket \mathbf{u}^\tau \rrbracket|_{\Gamma_\kappa}, \mathbf{u}^\tau|_{\partial \mathcal{D}_\kappa^o}) = \mathbf{0}.$$

In this setting, the unique continuation reads $\mathbf{u}^\tau = \mathbf{0}$, and thus, $\boldsymbol{\tau} = \mathbf{0}$ which concludes the proof. \square

Assumption 4.3. *Under Assumptions 2.2 and 2.3, one of the following applies:*

- $\mathfrak{R}(\mathbf{C}_\kappa - \mathbf{C}) - \alpha \mathfrak{I}(\mathbf{C}_\kappa)$ is positive definite on $\mathcal{D}_\kappa^* \setminus \overline{\Gamma_\kappa}$ for some constant $\alpha \geq 0$.
- For some constants $\alpha, \eta > 0$,

$$\overline{\mathbf{X}} : \mathfrak{R}(\mathbf{C} - \mathbf{C}_\kappa) : \mathbf{X} \geq \alpha |\mathbf{X}|^2, \quad \overline{\mathbf{X}} : \mathfrak{R}(\mathbf{C}_\kappa) : \mathbf{X} \geq \eta |\mathbf{X}|^2, \quad \|\mathfrak{I}(\mathbf{C}_\kappa)\|_{L^\infty} < \sqrt{\alpha \eta},$$

on $\mathcal{D}_\kappa^* \setminus \overline{\Gamma_\kappa}$ for all \mathbf{X} in $\mathbb{C}^{3 \times 3}$.

Lemma 4.6. *Under Assumptions 2.1, 2.2, 2.3, 4.2, and 4.3, the operator $T_\kappa : \mathfrak{S}(H_\Delta) \rightarrow \tilde{S}(\mathcal{D}_\kappa^* \cup \Gamma_\kappa \cup \partial \mathcal{D}_\kappa^o)$ is coercive, i.e., there exists a constant $c > 0$ independent of $\boldsymbol{\Xi}$ such that*

$$|\langle T_\kappa \boldsymbol{\Xi}, \boldsymbol{\Xi} \rangle| \geq c \|\boldsymbol{\Xi}\|_{\tilde{S}(\mathcal{D}_\kappa^* \cup \Gamma_\kappa \cup \partial \mathcal{D}_\kappa^o)}^2, \quad \forall \boldsymbol{\Xi} \in \mathfrak{S}(H_\Delta). \quad (29)$$

Proof. We adopt a contradiction argument as follows. Suppose (29) does not hold, then one may find a sequence $(\boldsymbol{\Xi}_n)_{n \in \mathbb{N}} \subset \mathfrak{S}(H_\Delta)$ such that

$$\|\boldsymbol{\Xi}_n\|_{\tilde{S}(\mathcal{D}_\kappa^* \cup \Gamma_\kappa \cup \partial \mathcal{D}_\kappa^o)} = 1, \quad |\langle T_\kappa \boldsymbol{\Xi}_n, \boldsymbol{\Xi}_n \rangle| \rightarrow 0 \quad \text{as } n \rightarrow \infty. \quad (30)$$

Denote by $\mathbf{v}^n \in H^1(\mathcal{B}_\kappa^- \cup \mathcal{D}_\kappa^* \setminus \overline{\Gamma_\kappa})^3$ the solution to (5) with

$$\begin{aligned} (\mathbf{u}^f|_{\mathcal{D}_\kappa^* \setminus \overline{\Gamma_\kappa}}, \nabla \mathbf{u}^f|_{\mathcal{D}_\kappa^* \setminus \overline{\Gamma_\kappa}}, \mathbf{t}[\mathbf{u}^f]|_{\Gamma_\kappa}, \mathbf{t}[\mathbf{u}^f]|_{\partial \mathcal{D}_\kappa^o}) &= \boldsymbol{\Xi}_n := \\ &\quad (\mathbf{u}^n|_{\mathcal{D}_\kappa^* \setminus \overline{\Gamma_\kappa}}, \nabla \mathbf{u}^n|_{\mathcal{D}_\kappa^* \setminus \overline{\Gamma_\kappa}}, \mathbf{t}[\mathbf{u}^n]|_{\Gamma_\kappa \cap \overline{\mathcal{D}_\kappa^*}} \oplus \boldsymbol{\psi}^n, \boldsymbol{\phi}^n), \\ \nabla \cdot \mathbf{C} : \nabla \mathbf{u}^n + \rho \omega^2 \mathbf{u}^n &= \mathbf{0} \text{ in } \mathcal{D}_\kappa^*, \quad (\boldsymbol{\psi}^n, \boldsymbol{\phi}^n) \in H^{-1/2}(\Gamma_\kappa \setminus \overline{\mathcal{D}_\kappa^*})^3 \times H^{-1/2}(\partial \mathcal{D}_\kappa^o)^3. \end{aligned}$$

Elliptic regularity implies that $\|\mathbf{v}^n\|_{H^2(\mathcal{B}_\kappa^-)^3}$ is bounded uniformly with respect to n . Then, up to changing the initial sequence, one may assume that $\boldsymbol{\Xi}_n$ weakly converges to some $\boldsymbol{\Xi}$ in

$S(\mathcal{D}_\kappa^* \cup \Gamma_\kappa \cup \partial\mathcal{D}_\kappa^o)$ and \mathbf{v}^n converges weakly in $H^2(\mathcal{B}_\kappa^-)^3 \cap H^1(\mathcal{D}_\kappa^* \setminus \overline{\Gamma_\kappa})^3$ to some $\mathbf{v} \in H^2(\mathcal{B}_\kappa^-)^3 \cap H^1(\mathcal{D}_\kappa^* \setminus \overline{\Gamma_\kappa})^3$. Now, observe that \mathbf{v} satisfies (5) for

$$\Xi = (\mathbf{u}|_{\mathcal{D}_\kappa^* \setminus \overline{\Gamma_\kappa}}, \nabla \mathbf{u}|_{\mathcal{D}_\kappa^* \setminus \overline{\Gamma_\kappa}}, \mathbf{t}[\mathbf{u}]|_{\Gamma_\kappa \cap \overline{\mathcal{D}_\kappa^*}} \oplus \boldsymbol{\psi}, \boldsymbol{\phi}), \quad (\boldsymbol{\psi}, \boldsymbol{\phi}) \in H^{-1/2}(\Gamma_\kappa \setminus \overline{\mathcal{D}_\kappa^*})^3 \times H^{-1/2}(\partial\mathcal{D}_\kappa^o)^3,$$

wherein $\nabla \cdot \mathbf{C} : \nabla \mathbf{u} + \rho\omega^2 \mathbf{u} = \mathbf{0}$ in \mathcal{D}_κ^* . In this setting, (26) along with $|\langle T_\kappa \Xi_n, \Xi_n \rangle| \rightarrow 0$ imply that $[[\mathbf{v}^n]] \rightarrow \mathbf{0}$ on Γ_κ and $\nabla(\mathbf{u}^n + \mathbf{v}^n) \rightarrow \mathbf{0}$ in $\mathcal{D}_\kappa^* \setminus \overline{\Gamma_\kappa}$, whereby the first of (5) reads that $\mathbf{u}^n + \mathbf{v}^n \rightarrow \mathbf{0}$ in $\mathcal{D}_\kappa^* \setminus \overline{\Gamma_\kappa}$. One may then deduce from the unique continuation principle that the total field $\mathbf{u}^n + \mathbf{v}^n$ also vanishes in \mathcal{B}_κ^- . In which case, (9) indicates that $\mathbf{v}^n \rightarrow \mathbf{0}$, and thus $\mathbf{v} = \mathbf{0}$, on $\partial\mathcal{B}_t$. This implies that (a) $\boldsymbol{\psi} = \boldsymbol{\phi} = \mathbf{0}$ by virtue of the second and fifth of (5) and the unique continuation, and (b) $\mathbf{u} = \mathbf{v} = \mathbf{0}$ which follows from Assumption 4.2.

Next, on recalling (16) and (17), (30) may be recast as

$$\begin{aligned} \langle T_\kappa \Xi_n, \Xi_n \rangle &= - \int_{\mathcal{D}_\kappa^* \setminus \overline{\Gamma_\kappa}} [\nabla \bar{\mathbf{u}}^n : (\mathbf{C}_\kappa - \mathbf{C}) : \nabla(\mathbf{u}^n + \mathbf{v}^n) + \omega^2(\rho - \rho_\kappa) \bar{\mathbf{u}}^n \cdot (\mathbf{u}^n + \mathbf{v}^n)] dV + \\ &\int_{\Gamma_\kappa \cap \overline{\mathcal{D}_\kappa^*}} \bar{\mathbf{t}}[\mathbf{u}^n] \cdot [[\mathbf{v}^n]] dS + \int_{\Gamma_\kappa \setminus \overline{\mathcal{D}_\kappa^*}} \bar{\boldsymbol{\psi}}^n \cdot [[\mathbf{v}^n]] dS + \int_{\partial\mathcal{D}_\kappa^o} \bar{\boldsymbol{\phi}}^n \cdot (\mathbf{u}_\phi^n + \mathbf{v}^n) dS. \end{aligned} \quad (31)$$

where \mathbf{u}_ϕ^n solves

$$\begin{aligned} \nabla \cdot \mathbf{C} : \nabla \mathbf{u}_\phi^n(\boldsymbol{\xi}) + \rho\omega^2 \mathbf{u}_\phi^n(\boldsymbol{\xi}) &= \mathbf{0}, & \boldsymbol{\xi} \in \mathcal{D}_\kappa^o, \\ \mathbf{n} \cdot \mathbf{C} : \nabla \mathbf{u}_\phi^n(\boldsymbol{\xi}) &= \boldsymbol{\phi}^n(\boldsymbol{\xi}), & \boldsymbol{\xi} \in \partial\mathcal{D}_\kappa^o. \end{aligned} \quad (32)$$

In addition, the variational form (61) with $\mathbf{v}^\kappa = \mathbf{v}' = \mathbf{v}^n$ reads

$$\begin{aligned} &\int_{\mathcal{D}_\kappa^* \setminus \overline{\Gamma_\kappa}} [\nabla \bar{\mathbf{v}}^n : (\mathbf{C}_\kappa - \mathbf{C}) : \nabla(\mathbf{u}^n + \mathbf{v}^n) + \omega^2(\rho - \rho_\kappa) \bar{\mathbf{v}}^n \cdot (\mathbf{u}^n + \mathbf{v}^n)] dV - \\ &- \int_{\Gamma_\kappa \cap \overline{\mathcal{D}_\kappa^*}} \mathbf{t}[\mathbf{u}^n] \cdot [[\bar{\mathbf{v}}^n]] dS - \int_{\Gamma_\kappa \setminus \overline{\mathcal{D}_\kappa^*}} \boldsymbol{\psi}^n \cdot [[\bar{\mathbf{v}}^n]] dS - \int_{\partial\mathcal{D}_\kappa^o} \boldsymbol{\phi}^n \cdot \bar{\mathbf{v}}^n dS = \\ &- \int_{\mathcal{B}_\kappa^- \cup \mathcal{D}_\kappa^* \setminus \overline{\Gamma_\kappa}} [\nabla \bar{\mathbf{v}}^n : \mathbf{C} : \nabla \mathbf{v}^n - \rho\omega^2 \bar{\mathbf{v}}^n \cdot \mathbf{v}^n] dV - \int_{\Gamma_\kappa} [[\bar{\mathbf{v}}^n]] \cdot \mathbf{K}_\kappa [[\mathbf{v}^n]] dS. \end{aligned} \quad (33)$$

Since $|\langle T_\kappa \Xi_n, \Xi_n \rangle| \rightarrow 0$ as $n \rightarrow \infty$, (31) in light of the Rellich compact embedding theorem along with the regularity of the trace operator implies that

$$\int_{\mathcal{D}_\kappa^* \setminus \overline{\Gamma_\kappa}} \nabla \bar{\mathbf{u}}^n : (\mathbf{C}_\kappa - \mathbf{C}) : \nabla(\mathbf{u}^n + \mathbf{v}^n) dV \rightarrow 0 \quad \text{as } n \rightarrow \infty. \quad (34)$$

Similarly, the compact embedding and trace theorems applied to (33) reads

$$\int_{\mathcal{D}_\kappa^* \setminus \overline{\Gamma_\kappa}} \nabla \bar{\mathbf{v}}^n : (\mathbf{C}_\kappa - \mathbf{C}) : \nabla(\mathbf{u}^n + \mathbf{v}^n) dV + \int_{\mathcal{B}_\kappa^- \cup \mathcal{D}_\kappa^* \setminus \overline{\Gamma_\kappa}} \nabla \bar{\mathbf{v}}^n : \mathbf{C} : \nabla \mathbf{v}^n dV \rightarrow 0 \quad (35)$$

as $n \rightarrow \infty$. On superimposing (34) and (35), one finds

$$\int_{\mathcal{D}_\kappa^* \setminus \overline{\Gamma_\kappa}} \nabla(\bar{\mathbf{u}}^n + \bar{\mathbf{v}}^n) : (\mathbf{C}_\kappa - \mathbf{C}) : \nabla(\mathbf{u}^n + \mathbf{v}^n) dV + \int_{\mathcal{B}_\kappa^- \cup \mathcal{D}_\kappa^* \setminus \overline{\Gamma_\kappa}} \nabla \bar{\mathbf{v}}^n : \mathbf{C} : \nabla \mathbf{v}^n dV \rightarrow 0$$

as $n \rightarrow \infty$. Now, following the first of Assumption 4.3, where $\Re(\mathbf{C}_\kappa - \mathbf{C}) - \alpha \Im(\mathbf{C}_\kappa)$ is positive definite on $\mathcal{D}_\kappa^* \setminus \overline{\Gamma_\kappa}$ for some constant $\alpha \geq 0$, observe that

$$\left| \int_{\mathcal{D}_\kappa^* \setminus \overline{\Gamma_\kappa}} \nabla(\bar{\mathbf{u}}^n + \bar{\mathbf{v}}^n) : (\mathbf{C}_\kappa - \mathbf{C}) : \nabla(\mathbf{u}^n + \mathbf{v}^n) dV + \int_{\mathcal{B}_\kappa^- \cup \mathcal{D}_\kappa^* \setminus \overline{\Gamma_\kappa}} \nabla \bar{\mathbf{v}}^n : \mathbf{C} : \nabla \mathbf{v}^n dV \right| \geq \theta \left(\int_{\mathcal{D}_\kappa^* \setminus \overline{\Gamma_\kappa}} |\nabla(\mathbf{u}^n + \mathbf{v}^n)|^2 dV + \int_{\mathcal{B}_\kappa^- \cup \mathcal{D}_\kappa^* \setminus \overline{\Gamma_\kappa}} |\nabla \mathbf{v}^n|^2 dV \right) \quad (36)$$

for some $\theta > 0$ independent of n . This implies that $\mathbf{v}^n \rightarrow \mathbf{0}$ strongly in $H^1(\mathcal{B}_\kappa^- \cup \mathcal{D}_\kappa^* \setminus \overline{\Gamma_\kappa})^3$ which is a contradiction. Given (34) and (35), the argument for establishing (29) for the second case of Assumption 4.3 directly follows the proof of Theorem 2.42 in [18]. \square

Lemma 4.7. *Under Assumptions 4.2 and 4.3, the real part of operator $T_\kappa : \mathfrak{S}(H_\Delta) \rightarrow \tilde{\mathfrak{S}}(\mathcal{D}_\kappa^* \cup \Gamma_\kappa \cup \partial \mathcal{D}_\kappa^o)$ may be decomposed on $\mathfrak{S}(H_\Delta)$ into a coercive part T_κ^\pm and a compact part T_c .*

Proof. See Appendix B. \square

Lemma 4.8. *The scattering operator $\Lambda_\kappa : L^2(\partial \mathcal{B}_t)^3 \rightarrow L^2(\partial \mathcal{B}_t)^3$ is injective, compact and has a dense range.*

Proof. The injectivity (resp. compactness) of $\Lambda_\kappa = \mathcal{V}_\kappa \mathcal{S}_\kappa$ results from the injectivity (resp. compactness) of \mathcal{V}_κ and \mathcal{S}_κ as per Lemmas 4.6 and 4.2. Now, according to Lemmas 4.3 and 4.6, the adjoint operators \mathcal{S}_κ^* , \mathcal{V}_κ^* , and thus $\Lambda_\kappa^* = \mathcal{S}_\kappa^* \mathcal{V}_\kappa^*$ are injective which establish the denseness of the range of Λ_κ . \square

5 Design of imaging functionals

Let us generate a set of sampling points $\mathbf{x}_o \in \mathcal{B}$ in the baseline model designating the loci of (monopole and dipole) trial scatterers. Monopole signatures are created via point sources applied along a set of trial directions \mathbf{n} , while dipole patterns are constructed by nucleating dislocations $L := \mathbf{x}_o + \mathbf{RL} \subset \mathcal{B}$ in the baseline model wherein \mathbf{L} is a smooth arbitrary-shaped discontinuity whose orientation is given by the unitary rotation matrix $\mathbf{R} \in U(3)$. In this setting, the scattering pattern $\Psi^o : \tilde{H}^{1/2}(L)^3 \rightarrow L^2(\partial \mathcal{B}_t)^3$ is defined by

$$\Psi^o(\boldsymbol{\xi}) := (1 - o) \mathbf{n} \cdot \mathbf{G}(\boldsymbol{\xi}, \mathbf{x}_o) + o \int_L \mathbf{a}(\mathbf{y}) \cdot \mathbf{T}(\boldsymbol{\xi}, \mathbf{y}) dS_{\mathbf{y}}, \quad o \in \{0, 1\}, \quad \boldsymbol{\xi} \in \partial \mathcal{B}_t, \quad (37)$$

for any admissible density $\mathbf{a} \in \tilde{H}^{1/2}(L)^3$. Keep in mind that the Green's dyadic \mathbf{G} satisfies (10) and its affiliated traction \mathbf{T} on L is specified in (9).

To construct a sampling-based imaging functional, we deploy Ψ^o to explore the range of Λ_κ by minimizing the below sequence of cost functions

$$\mathfrak{J}_\kappa^\gamma(\Psi^o; \boldsymbol{\tau}) := \|\Lambda_\kappa \boldsymbol{\tau} - \Psi^o\|_{L^2(\partial \mathcal{B}_t)}^2 + \gamma (\boldsymbol{\tau}, \Lambda_{\kappa_\#} \boldsymbol{\tau})_{L^2(\partial \mathcal{B}_t)}, \quad \boldsymbol{\tau} \in L^2(\partial \mathcal{B}_t)^3, \quad \gamma > 0, \quad (38)$$

where $\Lambda_{\kappa_\#} : L^2(\partial \mathcal{B}_t)^3 \rightarrow L^2(\partial \mathcal{B}_t)^3$ is given by

$$\Lambda_{\kappa_\#} := \frac{1}{2} |\Lambda_\kappa + \Lambda_\kappa^*| + \frac{1}{2i} (\Lambda_\kappa - \Lambda_\kappa^*). \quad (39)$$

Remark 5.1. Lemmas 4.3, 4.4, 4.5, 4.7 establish the premises of [36, Theorem 2.15] which concludes that operator $\Lambda_{\kappa_{\sharp}}$ is positive and has the following factorization

$$\Lambda_{\kappa_{\sharp}} = \mathcal{S}_{\kappa}^* T_{\kappa_{\sharp}} \mathcal{S}_{\kappa}, \quad (40)$$

where the middle operator $T_{\kappa_{\sharp}}$ is selfadjoint and positively coercive, i.e., there exists a constant $c > 0$ independent of Ξ so that

$$\langle T_{\kappa_{\sharp}} \Xi, \Xi \rangle \geq c \|\Xi\|_{S(\mathcal{D}_{\kappa}^* \cup \Gamma_{\kappa} \cup \partial \mathcal{D}_{\kappa}^o)}^2, \quad \forall \Xi \in \mathfrak{S}(H_{\Delta}). \quad (41)$$

Moreover, the range of \mathcal{S}_{κ}^* coincides with that of $\Lambda_{\kappa_{\sharp}}^{1/2}$.

Assumptions and lemmas of Section B furnish all the necessary conditions for the fundamental theorems of GLSM [6, 50] to apply. These results are required for the differential imaging indicators which for future reference are included in the following.

Theorem 5.1 ([6, 50]). Consider the minimizing sequence $\tau^{\gamma} \in L^2(\partial \mathcal{B}_t)^3$ for $\mathfrak{J}_{\kappa}^{\gamma}$ such that

$$\mathfrak{J}_{\kappa}^{\gamma}(\Psi^o; \tau^{\gamma}) \leq j_{\kappa}^{\gamma}(\Psi^o) + \eta(\gamma), \quad \gamma > 0, \quad (42)$$

where $\eta(\gamma)/\gamma \rightarrow 0$ as $\gamma \rightarrow 0$ and

$$j_{\kappa}^{\gamma}(\Psi^o) := \inf_{\tau \in L^2(\partial \mathcal{B}_t)^3} \mathfrak{J}_{\kappa}^{\gamma}(\Psi^o; \tau).$$

Then,

$$\begin{aligned} \Psi^o \in \text{Range}(\mathcal{V}_{\kappa}) &\Rightarrow \lim_{\gamma \rightarrow 0} (\tau^{\gamma}, \Lambda_{\kappa_{\sharp}} \tau^{\gamma}) < \infty, \\ \Psi^o \notin \text{Range}(\mathcal{V}_{\kappa}) &\Rightarrow \liminf_{\gamma \rightarrow 0} (\tau^{\gamma}, \Lambda_{\kappa_{\sharp}} \tau^{\gamma}) = \infty. \end{aligned} \quad (43)$$

Moreover, when $\mathcal{V}_{\kappa} \Xi = \Psi^o$, the sequence $\mathcal{S}_{\kappa} \tau^{\gamma}$ strongly converges to $\Xi \in \mathfrak{S}(H_{\Delta})$ as $\gamma \rightarrow 0$.

Corollary 5.1. Under Assumptions 2.4 and 4.2,

$$\Psi^o \in \text{Range}(\mathcal{V}_{\kappa}) \iff \mathbf{x}_o \in \mathcal{D}_{\kappa} \cup \Gamma_{\kappa}.$$

In addition, if

- $\mathbf{x}_o \in \mathcal{D}_{\kappa}^*$ then there exists a unique solution $(\mathbf{u}_{\kappa}^*, \mathbf{w}_{\kappa}^*)$ to

$$ITP_{\kappa} := ITP(\mathcal{D}_{\kappa}^*, \Gamma_{\kappa}; \{\mathbf{C}, \rho\}, \{\mathbf{C}_{\kappa}, \rho_{\kappa}\}, \mathbf{K}_{\kappa}; \mathbf{n} \cdot \mathbf{C} : \nabla \Psi^o, \Psi^o). \quad (44)$$

- $\mathbf{x}_o \in \mathcal{D}_{\kappa}^o$ then there exists a unique field \mathbf{u}_{κ}^o satisfying

$$\begin{aligned} \nabla \cdot (\mathbf{C} : \nabla \mathbf{u}_{\kappa}^o) + \rho \omega^2 \mathbf{u}_{\kappa}^o &= \mathbf{0} && \text{in } \mathcal{D}_{\kappa}^o, \\ \mathbf{n} \cdot \mathbf{C} : \nabla (\mathbf{u}_{\kappa}^o + \Psi^o) &= \mathbf{0} && \text{on } \partial \mathcal{D}_{\kappa}^o. \end{aligned} \quad (45)$$

- $L \subset \Gamma_{\kappa} \setminus \overline{\mathcal{D}_{\kappa}^*}$ then there exists a unique $[\mathbf{v}_{\kappa}] \in \tilde{H}^{1/2}(\Gamma_{\kappa} \setminus \overline{\mathcal{D}_{\kappa}^*})^3$ such that $\mathcal{S}_{\kappa}^* [\mathbf{v}_{\kappa}] = \Psi^1$. In this setting, the affiliated free-field traction $\mathbf{t}[\mathbf{u}_{\kappa}^f]$ may be obtained from the second of (5),

$$\mathbf{t}[\mathbf{u}_{\kappa}^f](\xi) = \mathbf{K}_{\kappa}(\xi)[\mathbf{v}_{\kappa}](\xi) - \mathbf{n} \cdot \mathbf{C} : \nabla \Psi^1(\xi), \quad \xi \in \Gamma_{\kappa} \setminus \overline{\mathcal{D}_{\kappa}^*}. \quad (46)$$

Now, let us recall from (1) that (a) $\mathcal{E}_i^* \subset \mathcal{B}$, $i \in \{1, 2, \dots\}$, is the support of (volumetric) elastic transformation where by Assumption 2.3 $\overline{\text{supp}(\mathbf{C}_i - \mathbf{C}_{i-1})} = \overline{\text{supp}(\rho_i - \rho_{i-1})}$, and $\mathcal{D}_i^* = \mathcal{E}_i^* \cup \mathcal{D}_{i-1}^*$ since $\overline{\mathcal{D}_{i-1}^*} \subset \mathcal{D}_i^*$, (b) \mathcal{E}_i^o designates the evolution of pore volume which is disjoint from \mathcal{E}_i^* since $\overline{\mathcal{D}_i^*} \cap \overline{\mathcal{D}_i^o} = \emptyset$, and (c) $\hat{\Gamma}_i \cup \tilde{\Gamma}_i$ represents the support of (geometric $\hat{\Gamma}_i$ and elastic $\tilde{\Gamma}_i$) interfacial evolution. On denoting by $\mathcal{D}_{i-1,j}^*$, $j = 1, 2, \dots, N_{i-1}$ (resp. $\mathcal{D}_{i,j}^*$, $j = 1, 2, \dots, N_i$) the simply connected components of \mathcal{D}_{i-1}^* (resp. \mathcal{D}_i^*), one may define the set of stationary inclusions

$$\tilde{\mathcal{D}}_{i-1}^* = \bigcup_{j \in \iota} \mathcal{D}_{i-1,j}^*, \quad \iota = \{j | \exists \mathcal{X} \mathcal{D}_{i-1,j}^* = \mathcal{D}_{i,\mathcal{X}}^* \wedge \overline{\mathcal{D}_{i-1,j}^*} \cap \overline{\mathcal{E}_i^*} \cup \overline{\hat{\Gamma}_i} \cup \overline{\tilde{\Gamma}_i} = \emptyset\}, \quad (47)$$

which remain unchanged between $[t_{i-1} \ t_i]$. By adopting a similar notation, the stationary pores are identified by

$$\tilde{\mathcal{D}}_{i-1}^o = \bigcup_{j \in \iota} \mathcal{D}_{i-1,j}^o, \quad \iota = \{j | \exists \mathcal{X} \mathcal{D}_{i-1,j}^o = \mathcal{D}_{i,\mathcal{X}}^o\}. \quad (48)$$

In this setting, $\tilde{\mathcal{D}}_{i-1}^\tau := \mathcal{D}_{i-1}^\tau \setminus \overline{\tilde{\mathcal{D}}_{i-1}^\tau}$, $\tau = \{\star, o\}$, signifies the evolved subset of \mathcal{D}_{i-1}^τ within the same timeframe. Further, one may introduce

$$\tilde{\mathcal{D}}_i^\tau = \bigcup_{j \in \tilde{\iota}} \mathcal{D}_{i,j}^\tau, \quad \tilde{\iota} = \{j | \overline{\mathcal{D}_{i,j}^\tau} \cap \overline{\tilde{\mathcal{D}}_{i-1}^\tau} \neq \emptyset\}, \quad \tau = \{\star, o\}, \quad (49)$$

so that \mathcal{E}_i^τ may be decomposed into disjoint subsets $\overline{\mathcal{E}_i^\tau} = \overline{\mathcal{E}_i^\tau} \cap \overline{\tilde{\mathcal{D}}_i^\tau}$ and $\hat{\mathcal{E}}_i^\tau = \mathcal{D}_i^\tau \setminus \{\tilde{\mathcal{D}}_{i-1}^\tau \cup \tilde{\mathcal{D}}_i^\tau\}$. Based in this, let us in addition define

$$\tilde{\Gamma}_{i-1} = \Gamma_{i-1} \setminus \overline{\hat{\Gamma}_i \cup \tilde{\mathcal{D}}_i^* \cup \mathcal{E}_i^* \cup \mathcal{E}_i^o}. \quad (50)$$

While our objective is to design imaging functionals to reconstruct $\mathcal{E}_i^* \cup \mathcal{E}_i^o \cup \hat{\Gamma}_i \cup \tilde{\Gamma}_i$ given sequential sensory data at t_{i-1} and t_i , one may observe in what follows that the proposed indicator is capable of recovering either $\tilde{\mathcal{D}}_{i-1}^* \cup \tilde{\mathcal{D}}_{i-1}^o \cup \tilde{\Gamma}_i$ or $\mathcal{E}_i^* \cup \mathcal{E}_i^o \cup \hat{\Gamma}_i \cup \tilde{\Gamma}_i \cup \tilde{\mathcal{D}}_{i-1}^* \cup \tilde{\mathcal{D}}_{i-1}^o$.

Assumption 5.1. Let us define $(\tilde{\mathbf{C}}, \tilde{\rho})$ in $\tilde{\mathcal{D}}_i^*$ by

$$(\tilde{\mathbf{C}}, \tilde{\rho})(\boldsymbol{\xi}) := \begin{cases} (\mathbf{C}_{i-1}, \rho_{i-1})(\boldsymbol{\xi}), & \boldsymbol{\xi} \in \tilde{\mathcal{D}}_{i-1}^* \\ (\mathbf{C}, \rho), & \boldsymbol{\xi} \in \tilde{\mathcal{D}}_i^* \setminus \tilde{\mathcal{D}}_{i-1}^* \end{cases}, \quad (51)$$

then $\omega > 0$ is not a transmission eigenvalue solving

$$\begin{aligned} & ITP_o^f(\tilde{\mathcal{E}}_i^*, \Gamma_{i-1}, \Gamma_i; \{\tilde{\mathbf{C}}, \tilde{\rho}\}, \{\mathbf{C}_i, \rho_i\}, \mathbf{K}_{i-1}, \mathbf{K}_i) := \\ & \left\{ \begin{array}{ll} \nabla \cdot [\mathbf{C}_i(\boldsymbol{\xi}) : \nabla \mathbf{w}_i^*](\boldsymbol{\xi}) + \rho_i(\boldsymbol{\xi}) \omega^2 \mathbf{w}_i^*(\boldsymbol{\xi}) = \mathbf{0}, & \boldsymbol{\xi} \in \tilde{\mathcal{E}}_i^* \setminus \overline{\Gamma}_i, \\ \nabla \cdot [\tilde{\mathbf{C}}(\boldsymbol{\xi}) : \nabla \tilde{\mathbf{w}}_i^*](\boldsymbol{\xi}) + \tilde{\rho}(\boldsymbol{\xi}) \omega^2 \tilde{\mathbf{w}}_i^*(\boldsymbol{\xi}) = \mathbf{0}, & \boldsymbol{\xi} \in \tilde{\mathcal{E}}_i^* \setminus \overline{\Gamma_{i-1}}, \\ \mathbf{t}[\mathbf{w}_i^*](\boldsymbol{\xi}) - \mathbf{t}[\tilde{\mathbf{w}}_i^*](\boldsymbol{\xi}) = \mathbf{0}, \quad [\mathbf{w}_i^* - \tilde{\mathbf{w}}_i^*](\boldsymbol{\xi}) = \mathbf{0}, & \boldsymbol{\xi} \in \partial \tilde{\mathcal{E}}_i^* \setminus \overline{\hat{\Gamma}_i} \cup \overline{\tilde{\Gamma}_i}, \\ \mathbf{t}[\mathbf{w}_i^*](\boldsymbol{\xi}) = \mathbf{K}_i(\boldsymbol{\xi})[\mathbf{w}_i^*](\boldsymbol{\xi}), \quad [\mathbf{t}[\mathbf{w}_i^*]](\boldsymbol{\xi}) = \mathbf{0}, & \boldsymbol{\xi} \in \Gamma_i \cap \tilde{\mathcal{E}}_i^*, \\ \mathbf{t}[\tilde{\mathbf{w}}_i^*](\boldsymbol{\xi}) = \mathbf{K}_{i-1}(\boldsymbol{\xi})[\tilde{\mathbf{w}}_i^*](\boldsymbol{\xi}), \quad [\mathbf{t}[\tilde{\mathbf{w}}_i^*]](\boldsymbol{\xi}) = \mathbf{0}, & \boldsymbol{\xi} \in \Gamma_{i-1} \cap \tilde{\mathcal{E}}_i^*, \\ \mathbf{t}[\mathbf{w}_i^*](\boldsymbol{\xi}) - \mathbf{t}[\tilde{\mathbf{w}}_i^*](\boldsymbol{\xi}) = \mathbf{0}, \quad \mathbf{t}[\mathbf{w}_i^*](\boldsymbol{\xi}) = \mathbf{K}_i(\boldsymbol{\xi})[\tilde{\mathbf{w}}_i^* - \mathbf{w}_i^*](\boldsymbol{\xi}), & \boldsymbol{\xi} \in \partial \tilde{\mathcal{E}}_i^* \cap \hat{\Gamma}_i, \\ \mathbf{t}[\mathbf{w}_i^*](\boldsymbol{\xi}) - \mathbf{t}[\tilde{\mathbf{w}}_i^*](\boldsymbol{\xi}) = \mathbf{0}, \quad (\mathbf{I} - \mathbf{K}_i \mathbf{K}_{i-1}^{-1}) \mathbf{t}[\mathbf{w}_i^*](\boldsymbol{\xi}) = \mathbf{K}_i(\boldsymbol{\xi})[\tilde{\mathbf{w}}_i^* - \mathbf{w}_i^*](\boldsymbol{\xi}), & \boldsymbol{\xi} \in \partial \tilde{\mathcal{E}}_i^* \cap \tilde{\Gamma}_i, \end{array} \right. \quad (52) \end{aligned}$$

Note that special cases such as elastic transformation or growth of intact inclusions are also included in (52) and may be obtained by setting $\Gamma_{i-1} = \emptyset$ and/or $\tilde{\Gamma}_i = \hat{\Gamma}_i = \emptyset$ in (52). Further, in the case of $\Gamma_{i-1} \cap \hat{\mathcal{E}}_i^* \neq \emptyset$, pertinent to the transformation of microcracked zones, it is further assumed that $\omega > 0$ does not satisfy $\text{ITP}_o^f(\hat{\mathcal{E}}_i^*, \Gamma_{i-1}, \Gamma_i; \{\mathbf{C}, \rho\}, \{\mathbf{C}_i, \rho_i\}, \mathbf{K}_{i-1}, \mathbf{K}_i)$.

Theorem 5.2. *Given Assumptions 2.4, 4.1, 4.2, 4.3, and 5.1,*

- Let $\mathbf{x}_o \in \mathcal{D}_{i-1}^*$ (or $L \subset \mathcal{D}_{i-1}^*$), then denote by $\mathbf{t}[\mathbf{u}_s^o]$ (resp. $\mathbf{t}[\mathbf{u}_s^f]$) the free-field traction on $\partial\mathcal{D}_s^o$ (resp. Γ_s) affiliated with the scattering pattern Ψ^o (or τ^γ), while $(\mathbf{u}_s^*, \mathbf{w}_s^*)$ uniquely solves ITP_s at times $t_s, s \in \{i-1, i\}$. In this setting,

If $\mathbf{x}_o \in \check{\mathcal{D}}_{i-1}^*$ (or $L \subset \check{\mathcal{D}}_{i-1}^*$) then

$$\begin{aligned} (\mathbf{u}_i^*|_{\mathcal{D}_{i-1}^* \setminus \overline{\Gamma_{i-1}}}, \nabla \mathbf{u}_i^*|_{\mathcal{D}_{i-1}^* \setminus \overline{\Gamma_{i-1}}}, \mathbf{t}[\mathbf{u}_i^f]|_{\Gamma_{i-1}}, \mathbf{t}[\mathbf{u}_i^o]|_{\partial\mathcal{D}_{i-1}^o}) = \\ (\mathbf{u}_{i-1}^*|_{\mathcal{D}_{i-1}^* \setminus \overline{\Gamma_{i-1}}}, \nabla \mathbf{u}_{i-1}^*|_{\mathcal{D}_{i-1}^* \setminus \overline{\Gamma_{i-1}}}, \mathbf{t}[\mathbf{u}_{i-1}^f]|_{\Gamma_{i-1}}, \mathbf{t}[\mathbf{u}_{i-1}^o]|_{\partial\mathcal{D}_{i-1}^o}). \end{aligned} \quad (53)$$

If $\mathbf{x}_o \in \tilde{\mathcal{D}}_{i-1}^*$ (or $L \subset \tilde{\mathcal{D}}_{i-1}^*$) then

$$\begin{aligned} (\mathbf{u}_i^*|_{\mathcal{D}_{i-1}^* \setminus \overline{\Gamma_{i-1}}}, \nabla \mathbf{u}_i^*|_{\mathcal{D}_{i-1}^* \setminus \overline{\Gamma_{i-1}}}, \mathbf{t}[\mathbf{u}_i^f]|_{\Gamma_{i-1} \cap \overline{\mathcal{D}_{i-1}^*}}) \neq \\ (\mathbf{u}_{i-1}^*|_{\mathcal{D}_{i-1}^* \setminus \overline{\Gamma_{i-1}}}, \nabla \mathbf{u}_{i-1}^*|_{\mathcal{D}_{i-1}^* \setminus \overline{\Gamma_{i-1}}}, \mathbf{t}[\mathbf{u}_{i-1}^f]|_{\Gamma_{i-1} \cap \overline{\mathcal{D}_{i-1}^*}}). \end{aligned} \quad (54)$$

- Provided that ω is not a Neumann eigenvalue of (45) per Assumption 4.1, then

If $\mathbf{x}_o \in \check{\mathcal{D}}_{i-1}^o$ (or $L \subset \check{\mathcal{D}}_{i-1}^o$) then (53) applies over $\mathcal{D}_{i-1}^* \cup \mathcal{D}_{i-1}^o \cup \Gamma_{i-1}$.
If $\mathbf{x}_o \in \tilde{\mathcal{D}}_{i-1}^o$ (or $L \subset \tilde{\mathcal{D}}_{i-1}^o$) then

$$\mathbf{t}[\mathbf{u}_i^o]|_{\partial\mathcal{D}_{i-1}^o} \neq \mathbf{t}[\mathbf{u}_{i-1}^o]|_{\partial\mathcal{D}_{i-1}^o}. \quad (55)$$

- Moreover,

If $L \subset \check{\Gamma}_{i-1}$ then (53) holds.
If $L \subset \Gamma_{i-1} \setminus \overline{\check{\Gamma}_{i-1} \cup \check{\mathcal{D}}_{i-1}^* \cup \tilde{\mathcal{D}}_{i-1}^*}$ then

$$\mathbf{t}[\mathbf{u}_i^f]|_{\Gamma_{i-1}} \neq \mathbf{t}[\mathbf{u}_{i-1}^f]|_{\Gamma_{i-1}}. \quad (56)$$

Proof. Let $\mathbf{x}_o \in \check{\mathcal{D}}_{i-1}^*$ (resp. $L \subset \check{\mathcal{D}}_{i-1}^*$), then observe that (a) Ψ^o (resp. Ψ^1) of (37) satisfies $\nabla \cdot \mathbf{C} : \nabla \Psi^o(\boldsymbol{\xi}) + \rho \omega^2 \Psi^o(\boldsymbol{\xi}) = \mathbf{0}$ in $\boldsymbol{\xi} \in \mathcal{D}_i \setminus \overline{\check{\mathcal{D}}_{i-1}^*}$ with $o = \{0, 1\}$, and thus, the solutions to ITP_s of (44) in $\mathcal{D}_s^* \setminus \overline{\check{\mathcal{D}}_{i-1}^*}$ is given by $(\mathbf{u}_s^*, \mathbf{w}_s^*) = (-\Psi^o, \mathbf{0})$ for $s = \{i, i-1\}$, (b) $\mathbf{t}[\mathbf{u}_s^o]|_{\partial\mathcal{D}_s^o} = -\mathbf{t}[\Psi^o]|_{\partial\mathcal{D}_s^o}$ in light of (a) and (45), and (c) in Corollary 5.1, $[[\mathbf{v}_s]] = \mathbf{0}$ on $\Gamma_s \setminus \overline{\check{\mathcal{D}}_{i-1}^*}$ which with reference to the contact law per the second of (5) implies $\mathbf{t}[\mathbf{u}_s^f]|_{\Gamma_s \setminus \overline{\check{\mathcal{D}}_{i-1}^*}} = -\mathbf{t}[\Psi^o]|_{\Gamma_s \setminus \overline{\check{\mathcal{D}}_{i-1}^*}}$. Further, note

from (44) and (47) that by definition $\text{ITP}_{i-1} = \text{ITP}_i$ in $\tilde{\mathcal{D}}_{i-1}^*$ so that

$$\begin{aligned} & (\mathbf{u}_{i-1}^* |_{\mathcal{D}_{i-1}^* \setminus \overline{\Gamma_{i-1}}}, \nabla \mathbf{u}_{i-1}^* |_{\mathcal{D}_{i-1}^* \setminus \overline{\Gamma_{i-1}}}, \mathbf{t}[\mathbf{u}_{i-1}^f] |_{\Gamma_{i-1}}, \mathbf{t}[\mathbf{u}_{i-1}^o] |_{\partial \mathcal{D}_{i-1}^o}) = \\ & \quad (\mathbf{u}_{i-1}^* |_{\tilde{\mathcal{D}}_{i-1}^* \setminus \overline{\Gamma_{i-1}}} \oplus -\Psi^o |_{\tilde{\mathcal{D}}_{i-1}^*}, \nabla \mathbf{u}_{i-1}^* |_{\tilde{\mathcal{D}}_{i-1}^* \setminus \overline{\Gamma_{i-1}}} \oplus -\nabla \Psi^o |_{\tilde{\mathcal{D}}_{i-1}^*}, \\ & \quad \mathbf{t}[\mathbf{u}_{i-1}^*] |_{\Gamma_{i-1} \cap \overline{\tilde{\mathcal{D}}_{i-1}^*}} \oplus -\mathbf{t}[\Psi^o] |_{\Gamma_{i-1} \setminus \overline{\tilde{\mathcal{D}}_{i-1}^*}}, -\mathbf{t}[\Psi^o] |_{\partial \mathcal{D}_{i-1}^o}), \\ & (\mathbf{u}_i^* |_{\mathcal{D}_i^* \setminus \overline{\Gamma_i}}, \nabla \mathbf{u}_i^* |_{\mathcal{D}_i^* \setminus \overline{\Gamma_i}}, \mathbf{t}[\mathbf{u}_i^f] |_{\Gamma_i}, \mathbf{t}[\mathbf{u}_i^o] |_{\partial \mathcal{D}_i^o}) = (\mathbf{u}_{i-1}^* |_{\tilde{\mathcal{D}}_{i-1}^* \setminus \overline{\Gamma_{i-1}}} \oplus -\Psi^o |_{\hat{\mathcal{D}}_i^* \cup \tilde{\mathcal{D}}_i^* \setminus \overline{\Gamma_i}}, \\ & \quad \nabla \mathbf{u}_{i-1}^* |_{\tilde{\mathcal{D}}_{i-1}^* \setminus \overline{\Gamma_{i-1}}} \oplus -\nabla \Psi^o |_{\hat{\mathcal{D}}_i^* \cup \tilde{\mathcal{D}}_i^* \setminus \overline{\Gamma_i}}, \mathbf{t}[\mathbf{u}_{i-1}^*] |_{\Gamma_{i-1} \cap \overline{\tilde{\mathcal{D}}_{i-1}^*}} \oplus -\mathbf{t}[\Psi^o] |_{\Gamma_i \setminus \overline{\tilde{\mathcal{D}}_{i-1}^*}}, -\mathbf{t}[\Psi^o] |_{\partial \mathcal{D}_i^o}), \end{aligned}$$

establishing (53). When $\mathbf{x}_o \in \tilde{\mathcal{D}}_{i-1}^o$ or $L \subset \tilde{\mathcal{D}}_{i-1}^o$, a similar argument leveraging (45) leads to

$$\begin{aligned} & (\mathbf{u}_s^* |_{\mathcal{D}_s^* \setminus \overline{\Gamma_s}}, \nabla \mathbf{u}_s^* |_{\mathcal{D}_s^* \setminus \overline{\Gamma_s}}, \mathbf{t}[\mathbf{u}_s^f] |_{\Gamma_s}, \mathbf{t}[\mathbf{u}_s^o] |_{\partial \mathcal{D}_s^o}) = (-\Psi^o |_{\mathcal{D}_s^* \setminus \overline{\Gamma_s}}, \\ & \quad -\nabla \Psi^o |_{\mathcal{D}_s^* \setminus \overline{\Gamma_s}}, -\mathbf{t}[\Psi^o] |_{\Gamma_s}, \mathbf{t}[\mathbf{u}_{i-1}^o] |_{\partial \tilde{\mathcal{D}}_{i-1}^o} \oplus -\mathbf{t}[\Psi^o] |_{\partial \mathcal{D}_s^o \setminus \partial \tilde{\mathcal{D}}_{i-1}^o}), \quad s \in \{i-1, i\}, \end{aligned}$$

which confirms (53). Same argument as above along with the proof of Theorem 4.5 in [50] leads to (53) when $L \subset \tilde{\Gamma}_{i-1}$.

Let $\mathbf{x}_o \in \tilde{\mathcal{D}}_{i-1}^*$ (or $L \subset \tilde{\mathcal{D}}_{i-1}^*$), then in light of the above observe that

$$\begin{aligned} & (\mathbf{u}_s^* |_{\mathcal{D}_s^* \setminus \overline{\tilde{\mathcal{D}}_s^* \cup \Gamma_s}}, \nabla \mathbf{u}_s^* |_{\mathcal{D}_s^* \setminus \overline{\tilde{\mathcal{D}}_s^* \cup \Gamma_s}}, \mathbf{t}[\mathbf{u}_s^f] |_{\Gamma_s \setminus \overline{\tilde{\mathcal{D}}_s^*}}, \mathbf{t}[\mathbf{u}_s^o] |_{\partial \mathcal{D}_s^o}) = \\ & \quad (-\Psi^o |_{\mathcal{D}_s^* \setminus \overline{\tilde{\mathcal{D}}_s^* \cup \Gamma_s}}, -\nabla \Psi^o |_{\mathcal{D}_s^* \setminus \overline{\tilde{\mathcal{D}}_s^* \cup \Gamma_s}}, -\mathbf{t}[\Psi^o] |_{\Gamma_s \setminus \overline{\tilde{\mathcal{D}}_s^*}}, -\mathbf{t}[\Psi^o] |_{\partial \mathcal{D}_s^o}), \quad s \in \{i-1, i\}. \end{aligned}$$

Next, a contradiction argument is adopted to analyze \mathbf{u}_s^* in $\tilde{\mathcal{D}}_s^*$, $s \in \{i-1, i\}$, as the following. Suppose that (54) does not hold i.e.,

$$\begin{aligned} & (\mathbf{u}_i^* |_{\tilde{\mathcal{D}}_{i-1}^* \setminus \overline{\Gamma_{i-1}}}, \nabla \mathbf{u}_i^* |_{\tilde{\mathcal{D}}_{i-1}^* \setminus \overline{\Gamma_{i-1}}}, \mathbf{t}[\mathbf{u}_i^f] |_{\Gamma_{i-1} \cap \overline{\tilde{\mathcal{D}}_{i-1}^*}}) = \\ & \quad (\mathbf{u}_{i-1}^* |_{\tilde{\mathcal{D}}_{i-1}^* \setminus \overline{\Gamma_{i-1}}}, \nabla \mathbf{u}_{i-1}^* |_{\tilde{\mathcal{D}}_{i-1}^* \setminus \overline{\Gamma_{i-1}}}, \mathbf{t}[\mathbf{u}_{i-1}^f] |_{\Gamma_{i-1} \cap \overline{\tilde{\mathcal{D}}_{i-1}^*}}), \end{aligned} \tag{57}$$

and consider the twelve generic configurations shown in Fig. 2 for microstructural evolution. The argument for similar or compound scenarios may be drawn from the following case studies. Keep in mind that the interior transmission problems of disconnected sets are independent. Based on this, $\tilde{\mathcal{D}}_{i-1}^*$, in each case, should be understood as the simply connected domain $\mathbf{x}_o \in \mathcal{D}_{i-1,j}^* \subset \tilde{\mathcal{D}}_{i-1}^*$ (or $\mathcal{D}_{i-1,j}^* \supset L$) as defined earlier.

Case 1–3 (fracturing of inclusions). With reference to Fig. 2 (a), consider the case where \mathbf{x}_o (or L) is in $\tilde{\mathcal{D}}_{i-1}^*$ where evolution occurs either by new internal/boundary fractures $\hat{\Gamma}_i$ or by elastically modified interfaces $\tilde{\Gamma}_i$. Under the premise of (57), let us define $\mathbf{w} = \mathbf{u}_i^* - \mathbf{u}_{i-1}^*$ in $\tilde{\mathcal{D}}_{i-1}^* \setminus \overline{\Gamma_i}$. On recalling (24), observe that the Cauchy data of \mathbf{w} vanishes on $\partial \tilde{\mathcal{D}}_{i-1}^* \setminus \overline{\Gamma_i}$ which implies by the unique continuation principle that $\mathbf{w} = \mathbf{0}$ in $\tilde{\mathcal{D}}_{i-1}^*$. In case 1 – where $\tilde{\mathcal{D}}_i^*$ is endowed with internal $\hat{\Gamma}_i$ – the contradiction arises from the discontinuity of \mathbf{w}_i^* across $\hat{\Gamma}_i$ while \mathbf{w}_{i-1}^* is continuous. The only exception to the latter, according to the fourth of (24), is when $\mathbf{t}[\mathbf{u}_i^*] = \mathbf{0}$ on $\hat{\Gamma}_i$ so that $\llbracket \mathbf{w}_i^* \rrbracket = \mathbf{0}$, which may not be the case per Assumption 4.1. In case 2 – where the

contact's elasticity \mathbf{K}_s with $s \in \{i-1, i\}$ changes over $\tilde{\Gamma}_i$ i.e., $\mathbf{K}_{i-1} \neq \mathbf{K}_i$ – vanishing \mathbf{w} in $\tilde{\mathcal{D}}_{i-1}^*$ implies $(\mathbf{K}_i - \mathbf{K}_{i-1})[[\mathbf{w}_i^*]] = (\mathbf{K}_i - \mathbf{K}_{i-1})[[\mathbf{w}_{i-1}^*]] = \mathbf{0}$ on $\tilde{\Gamma}_i$, by the fourth of (24), which requires $\mathbf{t}[\mathbf{w}_i^*] = \mathbf{t}[\mathbf{w}_{i-1}^*] = \mathbf{0}$ over $\tilde{\Gamma}_i$ that contradicts Assumption 4.1. In case 3 – where $\hat{\Gamma}_i \subset \partial\tilde{\mathcal{D}}_i^*$ – the contradiction may be observed from the fifth of (24) where $\mathbf{w} = \mathbf{0}$ reads $\mathbf{t}[\mathbf{w}_i^*] = \mathbf{0}$ on $\hat{\Gamma}_i$ with similar contradiction to Assumption 4.1.

Case 4 (evolution of elastic contacts). In this case where $L \subset \tilde{\Gamma}_i \setminus \overline{\mathcal{D}}_i^* \subset \Gamma_{i-1} \setminus \tilde{\Gamma}_{i-1}$, the fracture stiffness evolves within the matrix, as shown in Fig. 2 (a), such that $\mathbf{K}_i \neq \mathbf{K}_{i-1}$ on $\tilde{\Gamma}_i \setminus \overline{\mathcal{D}}_i^*$. Then, (56) is directly concluded from Theorem 4.5 and Theorem 4.7 of [50]. This may also be observed from (46).

Case 5 and 6 (volumetric growth or transformation of intact inclusions). The premise, as depicted in Fig. 2 (b), is that $\overline{\tilde{\mathcal{D}}_{i-1}^*} \cap \Gamma_i = \overline{\tilde{\mathcal{D}}_i^*} \cap \Gamma_i = \emptyset$. In this case, the contradiction to (57) may be argued similar to the proof of Theorem 4.2 in [6] which establishes (54).

Case 7–9 (elastic transformation or expansion of fractured inclusions). Let us define $\tilde{\mathbf{w}}_i^*$ in $\tilde{\mathcal{D}}_i^*$ as the following:

$$\tilde{\mathbf{w}}_i^*(\boldsymbol{\xi}) := \begin{cases} \mathbf{w}_{i-1}^*(\boldsymbol{\xi}), & \boldsymbol{\xi} \in \tilde{\mathcal{D}}_{i-1}^* \setminus \overline{\Gamma_{i-1}} \\ [\mathbf{u}_i^* + \boldsymbol{\Psi}^o](\boldsymbol{\xi}), & \boldsymbol{\xi} \in \tilde{\mathcal{D}}_i^* \setminus \overline{\tilde{\mathcal{D}}_{i-1}^*} \end{cases}, \quad (58)$$

Observe in light of (44) and (57) that $\tilde{\mathbf{w}}_i^*$ solves

$$\nabla \cdot \tilde{\mathbf{C}} : \nabla \tilde{\mathbf{w}}_i^* + \tilde{\rho} \omega^2 \tilde{\mathbf{w}}_i^* = \mathbf{0} \quad \text{in } \tilde{\mathcal{D}}_i^* \setminus \overline{\Gamma_{i-1}},$$

wherein $(\tilde{\mathbf{C}}, \tilde{\rho})$ is given by (51). In this setting, one may show that the Cauchy data affiliated with $\tilde{\mathbf{w}} = \tilde{\mathbf{w}}_i^* - \mathbf{w}_i^*$ vanish on $\partial\tilde{\mathcal{D}}_i^* \setminus \Gamma_i$ so that $(\mathbf{w}_i^*, \tilde{\mathbf{w}}_i^*)$ is the solution to $\text{ITP}_o^f(\tilde{\mathcal{D}}_i^*, \Gamma_{i-1}, \Gamma_i; \{\tilde{\mathbf{C}}, \tilde{\rho}\}, \{\mathbf{C}_i, \rho_i\}, \mathbf{K}_{i-1}, \mathbf{K}_i)$. To continue, let us consider two configurations: (cases 7, 8) where $\tilde{\mathcal{D}}_{i-1}^*$ is not included in any simply connected part $\tilde{\mathcal{E}}_{i,j}^*$ of $\tilde{\mathcal{E}}_i^*$, and (case 9) where $\tilde{\mathcal{D}}_{i-1}^* \subset \tilde{\mathcal{E}}_{i,j}^*$. Note that in cases 7, 8, $\partial\tilde{\mathcal{D}}_{i-1}^* \cap \partial\tilde{\mathcal{D}}_i^*$ is of nonzero surface measure, then owing to the equality of Cauchy data associated with $\tilde{\mathbf{w}}_i^*$ and \mathbf{w}_i^* and the fact that $(\mathbf{C}_i, \rho_i) = (\tilde{\mathbf{C}}, \tilde{\rho}) = (\mathbf{C}_{i-1}, \rho_{i-1})$ on $\partial\tilde{\mathcal{D}}_{i-1}^* \cap \partial\tilde{\mathcal{D}}_i^*$ one may conclude that $\tilde{\mathbf{w}}_i^* = \mathbf{w}_i^*$ on $\tilde{\mathcal{D}}_{i-1}^* \setminus \tilde{\mathcal{E}}_i^*$.

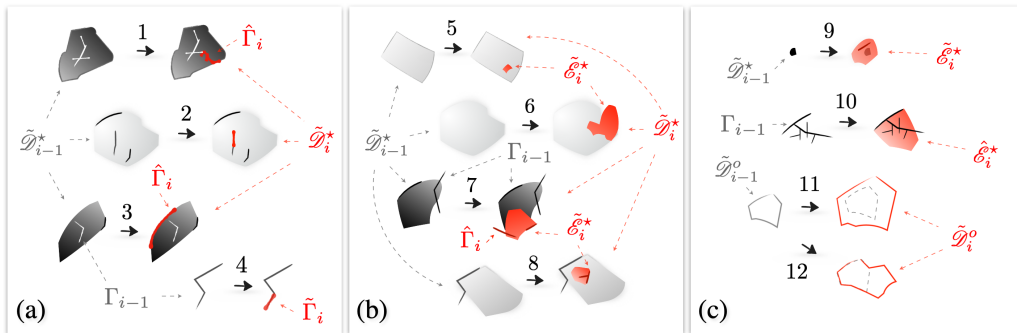


Figure 2: Twelve scenarios for microstructural transformation: (a) geometric expansion and/or elastic modification of discontinuity surfaces in inclusions or the binder, (b) new or modified (fractured) inclusions intersecting with previous (cracked) heterogeneities, and (c) newborn inclusions masking the microcracked damage zones and expansion of cavities.

Consequently, $(\mathbf{w}_i^*, \tilde{\mathbf{w}}_i^*)|_{\tilde{\mathcal{E}}_i^*}$ is the solution to $\text{ITP}_o^f(\tilde{\mathcal{E}}_i^*, \Gamma_{i-1}, \Gamma_i; \{\tilde{\mathbf{C}}, \tilde{\rho}\}, \{\mathbf{C}_i, \rho_i\}, \mathbf{K}_{i-1}, \mathbf{K}_i)$. The latter according to Assumption 5.1 implies that $\mathbf{w}_i^* = \tilde{\mathbf{w}}_i^* = \mathbf{0}$ in $\tilde{\mathcal{E}}_i^*$ which by unique continuation reads $\mathbf{w}_i^* = \mathbf{0}$ in $\tilde{\mathcal{D}}_i^*$. This requires $\mathbf{u}_i^* = -\Psi^o$ in $\tilde{\mathcal{D}}_{i-1}^*$ which is a contradiction since \mathbf{u}_i^* is smooth by definition while Ψ^o features a singularity at \mathbf{x}_o . In case 9, one may directly deduce from $\tilde{\mathcal{E}}_i^* \supset \tilde{\mathcal{E}}_{i,j}^* = \tilde{\mathcal{D}}_i^*$ and Assumption 5.1 that $\mathbf{w}_i^* = \mathbf{0}$ in $\tilde{\mathcal{D}}_i^*$ which leads to the same contradiction.

Case 10 (elastic transformation of microcracked damage zones). With reference to Fig. 2 (c), consider the case where L coincides with the binder's fractures at t_{i-1} ($L \subset \Gamma_{i-1}$) within a neighborhood that undergoes elastic evolution at t_i such that $L \subset \Gamma_{i-1} \cap \hat{\mathcal{E}}_i^*$. Contrary to (56), let

$$\mathbf{t}[\mathbf{u}_i^*]|_{\Gamma_{i-1} \cap \hat{\mathcal{E}}_i^*} = \mathbf{t}[\mathbf{u}_{i-1}^f]|_{\Gamma_{i-1} \cap \hat{\mathcal{E}}_i^*},$$

wherein both free fields \mathbf{u}_{i-1}^f and \mathbf{u}_i^* satisfy $\nabla \cdot \mathbf{C} : \nabla(\cdot) + \rho\omega^2(\cdot) = \mathbf{0}$ in $\hat{\mathcal{E}}_i^*$. Then observe that the latter also governs $\mathbf{u}^i = \mathbf{u}_i^* - \mathbf{u}_{i-1}^f$ such that $\mathbf{t}[\mathbf{u}^i] = \mathbf{0}$ on $\Gamma_{i-1} \cap \hat{\mathcal{E}}_i^*$, implying per Assumption 4.1 at t_{i-1} that $\mathbf{u}_i^* = \mathbf{u}_{i-1}^f$ in $\hat{\mathcal{E}}_i^*$. Based on which, one may define $\hat{\mathbf{w}}_i^* = \mathbf{u}_i^* + \Psi^1$ in $\hat{\mathcal{E}}_i^*$ and similar to Cases 7–9 conclude that $(\mathbf{w}_i^*, \hat{\mathbf{w}}_i^*)$ is a solution to $\text{ITP}_o^f(\hat{\mathcal{E}}_i^*, \Gamma_{i-1}, \Gamma_i; \{\mathbf{C}, \rho\}, \{\mathbf{C}_i, \rho_i\}, \mathbf{K}_{i-1}, \mathbf{K}_i)$, which by Assumption 5.1 reads $\hat{\mathbf{w}}_i^* = \mathbf{0}$ requiring that $\mathbf{u}_i^* = -\Psi^1$ in $\hat{\mathcal{E}}_i^*$ which is a contradiction since \mathbf{u}_i^* is smooth by definition while Ψ^1 has a discontinuity across L .

Case 11–12 (expansion of pores). Consider the case shown in Fig. 2 (c) where \mathbf{x}_o (or L) is in $\tilde{\mathcal{D}}_{i-1}^o$ where the evolution of cavities occurs. In contrast to (55), let

$$\mathbf{t}[\mathbf{u}_i^o]|_{\partial\mathcal{D}_{i-1}^o} = \mathbf{t}[\mathbf{u}_{i-1}^o]|_{\partial\mathcal{D}_{i-1}^o},$$

where \mathbf{u}_{i-1}^o , \mathbf{u}_i^o , and thus $\mathbf{u}^o = \mathbf{u}_i^o - \mathbf{u}_{i-1}^o$ satisfy $\nabla \cdot \mathbf{C} : \nabla(\cdot) + \rho\omega^2(\cdot) = \mathbf{0}$ in \mathcal{D}_{i-1}^o . Note that $\mathbf{t}[\mathbf{u}^o] = \mathbf{0}$ on $\partial\mathcal{D}_{i-1}^o$ implying per Assumption 4.1 that $\mathbf{u}_i^o = \mathbf{u}_{i-1}^o$ in \mathcal{D}_{i-1}^o . Keep in mind that \mathbf{u}_{i-1}^o (*resp.* \mathbf{u}_i^o) solves (45) in \mathcal{D}_{i-1}^o (*resp.* \mathcal{D}_i^o). Then, observe that $\mathbf{u}_i^o = -\Psi^o$ solves (45) within $\mathcal{D}_i^o \setminus \overline{\mathcal{D}_{i-1}^o}$ provided that $\mathbf{u}_i^o = \mathbf{u}_{i-1}^o$ in \mathcal{D}_{i-1}^o . In this setting, the continuity of \mathbf{u}_i^o across $\partial\mathcal{D}_{i-1}^o \setminus \partial\mathcal{D}_i^o$ along with the unique continuation principle require that $\mathbf{u}_i^o = -\Psi^o$ in \mathcal{D}_{i-1}^o which is a contradiction since \mathbf{u}_i^o is smooth according to (45) while Ψ^o has either a singularity at \mathbf{x}_o , or a discontinuity across L per (37). \square

Theorem 5.2 furnishes the main results required to (a) identify the invariants of scattering solutions according to Theorem 59 which is directly obtained by drawing from [6, Theorem 4.3] and [50, Theorem 4.7], and (b) establish the validity of differential evolution indicators in (60) following [6, Corollary 1].

Theorem 5.3. *Define*

$$\chi_i(\mathcal{G}_{i-1}, \mathcal{G}_i) := (\mathcal{G}_i - \mathcal{G}_{i-1}, \Lambda_{i-1\#}(\mathcal{G}_i - \mathcal{G}_{i-1})), \quad \mathcal{G}_{i-1}, \mathcal{G}_i \in L^2(\Omega)^3, \quad (59)$$

where $(\mathcal{G}_{i-1}, \mathcal{G}_i)(\Psi^o; \gamma)$ are the constructed minimizers of $(\mathfrak{J}_{i-1}^\gamma, \mathfrak{J}_i^\gamma)$ in (38) according to (42). Then, in light of factorization (12) and (13), Theorem 5.2 reads

$$\bullet \text{ If } \begin{cases} L \subset \tilde{\mathcal{D}}_{i-1}^* \cup \tilde{\mathcal{D}}_{i-1}^o \cup \tilde{\Gamma}_{i-1} \\ \mathbf{x}_o \in \tilde{\mathcal{D}}_{i-1}^* \cup \tilde{\mathcal{D}}_{i-1}^o \end{cases}, \text{ then } \lim_{\gamma \rightarrow 0} \chi_i[\mathcal{G}_{i-1}, \mathcal{G}_i](\Psi^o; \gamma) = 0.$$

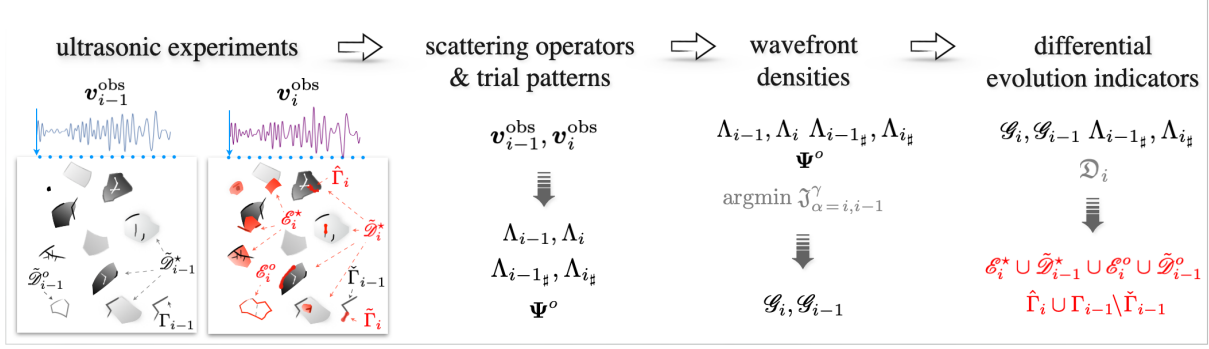


Figure 3: Differential imaging of evolution from sequential waveform data.

- If $\begin{cases} L \subset \tilde{\mathcal{D}}_{i-1}^* \cup \tilde{\mathcal{D}}_{i-1}^o \cup \Gamma_{i-1} \setminus \check{\Gamma}_{i-1} \\ \mathbf{x}_o \in \tilde{\mathcal{D}}_{i-1}^* \cup \tilde{\mathcal{D}}_{i-1}^o \end{cases}$, then $0 < \lim_{\gamma \rightarrow 0} \chi_i[\mathcal{G}_{i-1}, \mathcal{G}_i](\Psi^o; \gamma) < \infty$.
- If $\begin{cases} L \subset \mathcal{E}_i^* \setminus \overline{\tilde{\mathcal{D}}_{i-1}^*} \cup \mathcal{E}_i^o \setminus \overline{\tilde{\mathcal{D}}_{i-1}^o} \cup \hat{\Gamma}_i \setminus \overline{\tilde{\mathcal{D}}_{i-1}^*} \\ \mathbf{x}_o \in \mathcal{E}_i^* \setminus \overline{\tilde{\mathcal{D}}_{i-1}^*} \cup \mathcal{E}_i^o \setminus \overline{\tilde{\mathcal{D}}_{i-1}^o} \end{cases}$, then $\lim_{\gamma \rightarrow 0} \chi_i[\mathcal{G}_{i-1}, \mathcal{G}_i](\Psi^o; \gamma) = \infty$.

Differential evolution indicators. Let us introduce the imaging functionals $\mathfrak{D}_i : L^2(\Omega^3) \times L^2(\Omega^3) \rightarrow \mathbb{R}$ and $\tilde{\mathfrak{D}}_i : L^2(\Omega^3) \times L^2(\Omega^3) \rightarrow \mathbb{R}$ such that given $\Upsilon_i(\mathcal{G}_i) := (\mathcal{G}_i, \Lambda_{i\sharp} \mathcal{G}_i)$,

$$\begin{aligned} \mathfrak{D}_i(\mathcal{G}_{i-1}, \mathcal{G}_i) &:= \frac{1}{\sqrt{\Upsilon_i(\mathcal{G}_i) [1 + \Upsilon_i(\mathcal{G}_i) \chi_i^{-1}(\mathcal{G}_{i-1}, \mathcal{G}_i)]}}, \\ \tilde{\mathfrak{D}}_i(\mathcal{G}_{i-1}, \mathcal{G}_i) &:= \frac{1}{\sqrt{\Upsilon_{i-1}(\mathcal{G}_{i-1}) + \Upsilon_i(\mathcal{G}_i) [1 + \Upsilon_{i-1}(\mathcal{G}_{i-1}) \chi_i^{-1}(\mathcal{G}_{i-1}, \mathcal{G}_i)]}}. \end{aligned} \quad (60)$$

Then, it follows that

- $\begin{cases} L \subset \mathcal{E}_i^* \cup \tilde{\mathcal{D}}_{i-1}^* \cup \mathcal{E}_i^o \cup \tilde{\mathcal{D}}_{i-1}^o \cup \hat{\Gamma}_i \cup \Gamma_{i-1} \setminus \check{\Gamma}_{i-1} \\ \mathbf{x}_o \in \mathcal{E}_i^* \cup \tilde{\mathcal{D}}_{i-1}^* \cup \mathcal{E}_i^o \cup \tilde{\mathcal{D}}_{i-1}^o \end{cases} \iff \lim_{\gamma \rightarrow 0} \mathfrak{D}_i(\mathcal{G}_{i-1}, \mathcal{G}_i)(\Psi^o; \gamma) > 0.$
- $\begin{cases} L \subset \tilde{\mathcal{D}}_{i-1}^* \cup \tilde{\mathcal{D}}_{i-1}^o \cup \Gamma_{i-1} \setminus \check{\Gamma}_{i-1} \\ \mathbf{x}_o \in \tilde{\mathcal{D}}_{i-1}^* \cup \tilde{\mathcal{D}}_{i-1}^o \end{cases} \iff \lim_{\gamma \rightarrow 0} \tilde{\mathfrak{D}}_i(\mathcal{G}_{i-1}, \mathcal{G}_i)(\Psi^o; \gamma) > 0.$

In other words, \mathfrak{D}_i (*resp.* $\tilde{\mathfrak{D}}_i$) assumes near-zero values except at the loci of $\tilde{\mathcal{D}}_{i-1}^* \cup \tilde{\mathcal{D}}_{i-1}^o \cup \Gamma_{i-1} \setminus \check{\Gamma}_{i-1}$ (*resp.* $\tilde{\mathcal{D}}_{i-1}^* \cup \tilde{\mathcal{D}}_{i-1}^o \cup \Gamma_{i-1} \setminus \check{\Gamma}_{i-1}$) where the indicator increases and remains finite as $\gamma \rightarrow 0$. By building on [6, Theorem 4.4] and [50, Theorem 4.8], it is quite straightforward to formulate pertinent results for noisy data which for brevity are not included in this paper. To summarize, Fig. 3 provides the steps for the construction of evolution indicators from numerical or laboratory test data.

6 Synthetic experiments

The evolution indicators of (60) are put to test in this section by a set of numerical experiments. The primary focus is on a randomly heterogeneous and discontinuous background with evolving microstructure due to elastic transformation and/or fracturing. The special cases of *monolithic* solids endowed with crack or pore networks are reported in [50]. In this section, the synthetic scattered fields $\mathbf{v}_i^{\text{obs}}$, $i = \{0, 1, 2, 3\}$, are simulated via the boundary element method [15], see [49] for more on the computational platform.

With reference to Fig. 4, the testing configuration at t_0 i.e., the background domain entails a composite slab of dimensions $2.5 \times 2.5 \times 0.01$ comprised of an elastic binder endowed with ellipsoidal inclusions of arbitrary distribution and size. The in-plane diameters of scatterers ranges from one to five shear wavelengths $\lambda_s = 0.04$, while their pairwise distances are greater than $2\lambda_s$. The normalized shear modulus, mass density, and Poisson's ratio of the matrix are taken as $\mu_m = 1$, $\rho_m = 1$ and $\nu_m = 0.25$, while that of the scatterers are $\mu_s = 2$, $\rho_s = \rho_m$ and $\nu_s = \nu_m$. In this setting, the shear and compressional wave speeds in the matrix are $c_m^s = 1$ and $c_m^p = 1.73$. The specimen's microstructural evolution in the following time steps $t_1 - t_3$, according to Fig. 4, involves (a) multi-step fracturing of the binder and inclusions and their coalescence, (b) elastic transformation of pre-existing inclusions at t_0 , and (c) emergence of new volumetric heterogeneities with shear modulus $\mu_s^{\text{new}} = 1.5$. Note the gradual increase in the evolution complexity, and in particular, the density of scatterers such that at t_3 : (a) the pairwise distance between scatterers may reduce to a small fraction of λ_s , and (b) a subset of evolution support is deeply embedded within the stationary scatterers.

Synthetic experiments are conducted at four time steps $t_0 - t_3$ when the specimen assumes the geometric configurations shown in Fig. 4. Every sensing step entails 2000 forward simulations where in-plane harmonic waves of frequency $\omega = 140$ rad/s are generated at a point source over the specimen's external boundary. The resulting scattered fields $\mathbf{v}_i^{\text{obs}}$, $i = \{0, 1, 2, 3\}$, are then calculated on the same grid by solving the 3D elastodynamics boundary integral equations. Given that λ_s is four times greater than the specimen thickness, the leading contributions to scattered fields are the in-plane components which are then used for data inversion.

The obtained scattered signatures are used to compute the synthetic wavefront densities \mathcal{G}_i , $i = \{0, 1, 2, 3\}$, as approximate minimizers of the cost functionals in (38). The latter follows the common three steps required for constructing any sampling-based indicator, namely: (1) forming the discrete scattering operators $\Lambda_{i_\#}$ at every t_i , (2) assembling the trial signatures Ψ^o of (37) as the right-hand side of the scattering equation, and (3) solving the latter by minimizing the discretized cost function (38) by invoking the Morozov discrepancy principle. A detailed account of this process is provided in [50]. Given $\Lambda_{i_\#}$ and \mathcal{G}_i , one may then evaluate the imaging functionals \mathfrak{D}_i from (60) which is expected to achieve its highest values at the loci of new and evolved scatterers in each sensing sequence.

Fig. 5 illustrates the successive evolution indicators \mathfrak{D}_j , $j = \{1, 2, 3\}$, over the sampling area. For each time window $t_{j-1} - t_j$, the "true" support of elastic variations is provided in the top

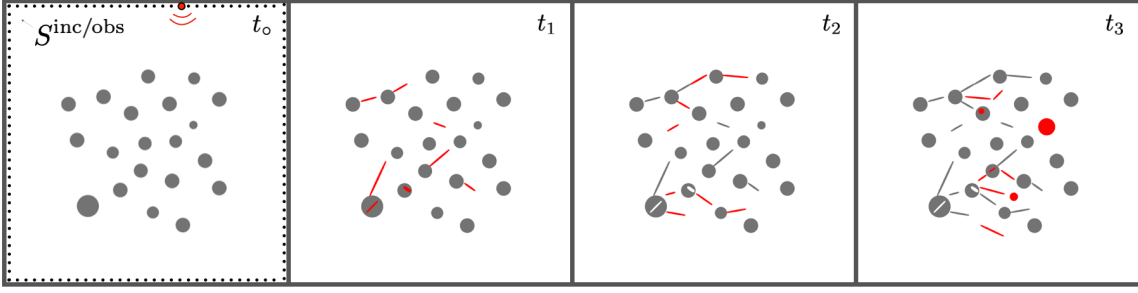


Figure 4: Microstructural geometry of a composite slab with evolving heterogeneities and discontinuities at four sensing steps $t_0 - t_3$. Elastic (in-plane) waves are periodically generated via boundary excitations on S^{inc} , and the affiliated scattered waveforms are computed over the observation surface S^{obs} . Here, $S^{\text{inc}} = S^{\text{obs}}$ is sampled at 10^3 points around the model perimeter.

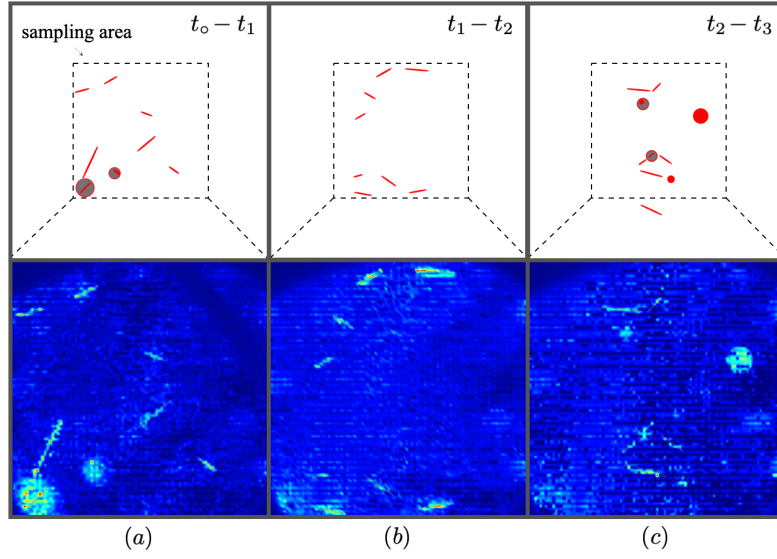


Figure 5: Three-step reconstruction of elastic and interfacial transformations (a-c) of the initial configuration shown in Fig. 4 (a): (top) evolution geometry in the sensing sequence $[t_{i-1} t_i]$, $i = \{1, 2, 3\}$, and (bottom) the affiliated indicator map \mathfrak{D}_i of (60) computed from the observed scattered field data $\mathbf{v}_{i-1}^{\text{obs}}$ and $\mathbf{v}_i^{\text{obs}}$.

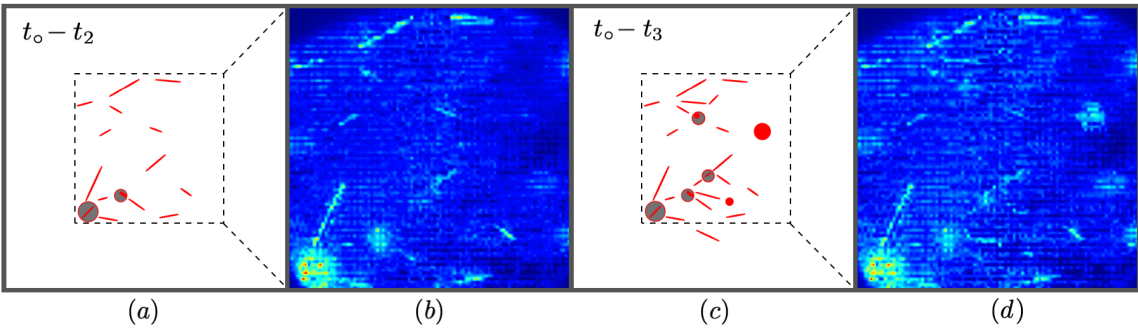


Figure 6: Multi-step reconstruction of elastic and geometric variations: (a), (c) true evolution support between $[t_0 t_2]$ and $[t_0 t_3]$ respectively, and (b), (d) the associated (superimposed) differential maps.

row. Keep in mind that in any sequence, \mathfrak{D}_j is by design insensitive to the scatterers at t_{j-1} provided that they remain unchanged by t_j . The differential maps within $t_o - t_2$ feature relatively sharp localizations with minimal artifacts which, given the shear wavelength, may be attributed to the rather sparse distribution of scatterers in this timeframe. Some artifacts emerge in the \mathfrak{D}_3 map, however, since the elastic variations between $t_2 - t_3$ occur within a densely packed network of fractures and inclusions which are assumed to be unknown. To recover the evolution support over an extended timeframe as the microstructure becomes progressively complex, one may superimpose the consecutive reconstructions (of Fig. 5) as in Fig. 6.

7 Conclusion

This study furnishes the theoretical foundation for differential evolution indicators for ultrasonic imaging of elastic variations within a heterogeneous and discontinuous background of random structure. In this vein, the wellposedness conditions for the forward and inverse scattering problems are established; in light of which, the pairwise relation between scattering solutions – associated with distinct datasets, is determined. For this purpose, twelve scenarios for microstructural transitions are investigated including (a) fracturing of inclusions, (b) evolution of discontinuity surfaces within each material component or at bimaterial interfaces, (c) elastic transformation and/or expansion of fractured inclusions, (d) conversion of microcracked damage zones, and (e) expansion of pores. In all cases, it is shown that certain measures of the synthetic incident fields constructed based on the scattering solutions are, in the limit, equivalent at the loci of unknown scatterers which remain both geometrically and mechanically invariant between a given pair of time steps. This allows for exclusive reconstruction of evolved features without the knowledge (or need for recovery) of stationary components in the background. This is particularly useful in uncertain environments as showcased by the synthetic experiments – provided that the illuminating wavelength is sufficiently smaller than the relevant microstructural length scales e.g., pairwise distance between the scatterers. Relaxing such constraints may be possible through time-domain inversion as a potential direction in future studies.

8 Acknowledgements

The corresponding author kindly acknowledges the support provided by the National Science Foundation (Grant No. 1944812). This work utilized resources from the University of Colorado Boulder Research Computing Group, which is supported by the National Science Foundation (awards ACI-1532235 and ACI-1532236), the University of Colorado Boulder, and Colorado State University.

A Wellposedness of the direct scattering problem

Observe that $\forall \mathbf{v}' \in H^1(\mathcal{B}_\kappa^- \cup \mathcal{D}_\kappa^* \setminus \overline{\Gamma_\kappa})^3$, the variational form of (5) reads

$$\begin{aligned} & \int_{\mathcal{B}_\kappa^-} [\nabla \bar{\mathbf{v}}' : \mathbf{C} : \nabla \mathbf{v}^\kappa - \rho \omega^2 \bar{\mathbf{v}}' \cdot \mathbf{v}^\kappa] dV_\xi + \int_{\Gamma_\kappa} \llbracket \bar{\mathbf{v}}' \rrbracket \cdot \mathbf{K}_\kappa \llbracket \mathbf{v}^\kappa \rrbracket dS_\xi + \\ & + \int_{\mathcal{D}_\kappa^* \setminus \overline{\Gamma_\kappa}} [\nabla \bar{\mathbf{v}}' : \mathbf{C}_\kappa : \nabla \mathbf{v}^\kappa - \rho_\kappa \omega^2 \bar{\mathbf{v}}' \cdot \mathbf{v}^\kappa] dV_\xi = \int_{\partial \mathcal{D}_\kappa^o} \bar{\mathbf{v}}' \cdot \mathbf{t}^f dS_\xi + \\ & + \int_{\mathcal{D}_\kappa^* \setminus \overline{\Gamma_\kappa}} [(\rho_\kappa - \rho) \omega^2 \bar{\mathbf{v}}' \cdot \mathbf{u}^f - \nabla \bar{\mathbf{v}}' : (\mathbf{C}_\kappa - \mathbf{C}) : \nabla \mathbf{u}^f] dV_\xi + \int_{\Gamma_\kappa} \llbracket \bar{\mathbf{v}}' \rrbracket \cdot \mathbf{t}^f dS_\xi. \end{aligned} \quad (61)$$

The sesquilinear form on the left-hand side of (61) may be decomposed as $A(\mathbf{v}^\kappa, \mathbf{v}') + B(\mathbf{v}^\kappa, \mathbf{v}')$ where

$$\begin{aligned} A(\mathbf{v}^\kappa, \mathbf{v}') &= \int_{\mathcal{D}_\kappa^* \setminus \overline{\Gamma_\kappa}} [\nabla \bar{\mathbf{v}}' : \mathbf{C}_\kappa : \nabla \mathbf{v}^\kappa + \bar{\mathbf{v}}' \cdot \mathbf{v}^\kappa] dV_\xi + \int_{\mathcal{B}_\kappa^-} [\nabla \bar{\mathbf{v}}' : \mathbf{C} : \nabla \mathbf{v}^\kappa + \bar{\mathbf{v}}' \cdot \mathbf{v}^\kappa] dV_\xi, \\ B(\mathbf{v}^\kappa, \mathbf{v}') &= -(1 + \rho_\kappa \omega^2) \int_{\mathcal{D}_\kappa^* \setminus \overline{\Gamma_\kappa}} \bar{\mathbf{v}}' \cdot \mathbf{v}^\kappa dV_\xi - (1 + \rho \omega^2) \int_{\mathcal{B}_\kappa^-} \bar{\mathbf{v}}' \cdot \mathbf{v}^\kappa dV_\xi + \\ & + \int_{\Gamma_\kappa} \llbracket \bar{\mathbf{v}}' \rrbracket \cdot \mathbf{K}_\kappa \llbracket \mathbf{v}^\kappa \rrbracket dS_\xi, \quad \forall \mathbf{v}' \in H^1(\mathcal{B}_\kappa^- \cup \mathcal{D}_\kappa^* \setminus \overline{\Gamma_\kappa})^3. \end{aligned} \quad (62)$$

In light of the Korn inequality [49], observe that $A(\mathbf{v}^\kappa, \mathbf{v}')$ is coercive. Moreover, the antilinear form $B(\mathbf{v}^\kappa, \mathbf{v}')$ is compact by the application of Cauchy–Schwarz inequality to $|B(\mathbf{v}^\kappa, \mathbf{v}')|$, the compact embedding of $H^1(\mathcal{B}_\kappa^- \cup \mathcal{D}_\kappa^* \setminus \overline{\Gamma_\kappa})^3$ into $L^2(\mathcal{B}_\kappa^- \cup \mathcal{D}_\kappa^* \setminus \overline{\Gamma_\kappa})^3$, and the compactness of the trace operator $\mathbf{v}^\kappa \rightarrow \llbracket \mathbf{v}^\kappa \rrbracket$ as a map from $H^1(\mathcal{B}_\kappa^- \cup \mathcal{D}_\kappa^* \setminus \overline{\Gamma_\kappa})^3$ to $L^2(\Gamma_\kappa)^3$ owing to the compact embedding of $\tilde{H}^{1/2}(\Gamma_\kappa)^3$ into $L^2(\Gamma_\kappa)^3$. As a result, (5) is of Fredholm type, and thus, is wellposed as soon as the uniqueness of a solution is guaranteed. Let $(\mathbf{u}^f|_{\mathcal{D}_\kappa^* \setminus \overline{\Gamma_\kappa}}, \nabla \mathbf{u}^f|_{\mathcal{D}_\kappa^* \setminus \overline{\Gamma_\kappa}}, \mathbf{t}[\mathbf{u}^f]|_{\Gamma_\kappa}, \mathbf{t}[\mathbf{u}^f]|_{\partial \mathcal{D}_\kappa^o}) = \mathbf{0}$, then on setting $\mathbf{v}' = \mathbf{v}^\kappa$, observe from (61) that

$$\Im \left(\int_{\mathcal{D}_\kappa^* \setminus \overline{\Gamma_\kappa}} \nabla \bar{\mathbf{v}}^\kappa : \mathbf{C}_\kappa : \nabla \mathbf{v}^\kappa dV_\xi + \int_{\Gamma_\kappa} \llbracket \bar{\mathbf{v}}^\kappa \rrbracket \cdot \mathbf{K}_\kappa \llbracket \mathbf{v}^\kappa \rrbracket dS_\xi \right) = 0,$$

implying that $\llbracket \mathbf{v}^\kappa \rrbracket = \mathbf{0}$ on Γ_κ , and $\mathbf{v}^\kappa = \mathbf{0}$ in $\mathcal{D}_\kappa^* \setminus \overline{\Gamma_\kappa}$ owing to Assumption 2.2 and the first of (5). Note that the jump in \mathbf{v}^κ vanishes not only on the intersection $\Gamma_\kappa \cap \partial \mathcal{D}_\kappa^*$, but also on the perfectly continuous interface $\partial \mathcal{D}_\kappa^* \setminus \overline{\Gamma_\kappa}$ according to the fourth of (5). Thus, the Holmgren’s theorem implies that the scattered field \mathbf{v}^κ vanishes in an open neighborhood of $\partial \mathcal{D}_\kappa^*$ which by virtue of the unique continuation theorem leads to $\mathbf{v}^\kappa(\boldsymbol{\xi}) = \mathbf{0}$ in $\boldsymbol{\xi} \in \mathcal{B} \setminus \overline{\mathcal{D}_\kappa^o}$. This completes the proof for the uniqueness of a scattering solution in $\mathcal{B}_\kappa^- \cup \mathcal{D}_\kappa^* \setminus \overline{\Gamma_\kappa}$, and thus, substantiates the wellposedness of the forward problem.

B Proof of Lemma 4.7

Let $\hat{\mathbf{v}}$ (*resp.* \mathbf{v}') satisfies (5) for

$$\mathbf{X} = (\hat{\mathbf{u}}|_{\mathcal{D}_\kappa^* \setminus \overline{\Gamma_\kappa}}, \nabla \hat{\mathbf{u}}|_{\mathcal{D}_\kappa^* \setminus \overline{\Gamma_\kappa}}, \mathbf{t}[\hat{\mathbf{u}}]|_{\Gamma_\kappa \cap \overline{\mathcal{D}_\kappa^*}} \oplus \boldsymbol{\psi}, \boldsymbol{\phi}), \quad (\boldsymbol{\psi}, \boldsymbol{\phi}) \in H^{-1/2}(\Gamma_\kappa \setminus \overline{\mathcal{D}_\kappa^*})^3 \times H^{-1/2}(\partial \mathcal{D}_\kappa^o)^3,$$

(resp.

$$\mathbf{X}' = (\mathbf{u}'|_{\mathcal{D}_\kappa^* \setminus \overline{\Gamma_\kappa}}, \nabla \mathbf{u}'|_{\mathcal{D}_\kappa^* \setminus \overline{\Gamma_\kappa}}, \mathbf{t}[\mathbf{u}']|_{\Gamma_\kappa \cap \overline{\mathcal{D}_\kappa^*}} \oplus \boldsymbol{\psi}', \boldsymbol{\phi}'), \quad (\boldsymbol{\psi}', \boldsymbol{\phi}') \in H^{-1/2}(\Gamma_\kappa \setminus \overline{\mathcal{D}_\kappa^*})^3 \times H^{-1/2}(\partial \mathcal{D}_\kappa^o)^3),$$

wherein $\nabla \cdot \mathbf{C} : \nabla \hat{\mathbf{u}} + \rho \omega^2 \hat{\mathbf{u}} = \mathbf{0}$ (resp. $\nabla \cdot \mathbf{C} : \nabla \mathbf{u}' + \rho \omega^2 \mathbf{u}' = \mathbf{0}$) in \mathcal{D}_κ^* , then

$$\begin{aligned} \langle T_\kappa \mathbf{X}, \mathbf{X}' \rangle &= - \int_{\mathcal{D}_\kappa^* \setminus \overline{\Gamma_\kappa}} [\nabla \bar{\mathbf{u}}' : (\mathbf{C}_\kappa - \mathbf{C}) : \nabla (\hat{\mathbf{u}} + \hat{\mathbf{v}}) + \omega^2 (\rho - \rho_\kappa) \bar{\mathbf{u}}' \cdot (\hat{\mathbf{u}} + \hat{\mathbf{v}})] dV + \\ & \int_{\Gamma_\kappa \cap \overline{\mathcal{D}_\kappa^*}} \bar{\mathbf{t}}[\mathbf{u}'] \cdot \llbracket \hat{\mathbf{v}} \rrbracket dS + \int_{\Gamma_\kappa \setminus \overline{\mathcal{D}_\kappa^*}} \bar{\boldsymbol{\psi}}' \cdot \llbracket \hat{\mathbf{v}} \rrbracket dS + \int_{\partial \mathcal{D}_\kappa^o} \bar{\boldsymbol{\phi}}' \cdot (\hat{\mathbf{u}}_\phi + \hat{\mathbf{v}}) dS, \end{aligned} \quad (63)$$

where $\hat{\mathbf{u}}_\phi$ satisfies (32) with $\boldsymbol{\phi}^n = \boldsymbol{\phi}$. In addition, the variational form (61) with $\mathbf{v}^\kappa = \hat{\mathbf{v}}$ and $\mathbf{v}' = \mathbf{v}'$ reads

$$\begin{aligned} & \int_{\mathcal{D}_\kappa^* \setminus \overline{\Gamma_\kappa}} [\nabla \bar{\mathbf{v}}' : (\mathbf{C}_\kappa - \mathbf{C}) : \nabla (\hat{\mathbf{u}} + \hat{\mathbf{v}}) + \omega^2 (\rho - \rho_\kappa) \bar{\mathbf{v}}' \cdot (\hat{\mathbf{u}} + \hat{\mathbf{v}})] dV - \\ & - \int_{\Gamma_\kappa \cap \overline{\mathcal{D}_\kappa^*}} \mathbf{t}[\hat{\mathbf{u}}] \cdot \llbracket \bar{\mathbf{v}}' \rrbracket dS - \int_{\Gamma_\kappa \setminus \overline{\mathcal{D}_\kappa^*}} \boldsymbol{\psi} \cdot \llbracket \bar{\mathbf{v}}' \rrbracket dS - \int_{\partial \mathcal{D}_\kappa^o} \boldsymbol{\phi} \cdot \bar{\mathbf{v}}' dS = \\ & - \int_{\mathcal{B}_\kappa^- \cup \mathcal{D}_\kappa^* \setminus \overline{\Gamma_\kappa}} [\nabla \bar{\mathbf{v}}' : \mathbf{C} : \nabla \hat{\mathbf{v}} - \rho \omega^2 \bar{\mathbf{v}}' \cdot \hat{\mathbf{v}}] dV - \int_{\Gamma_\kappa} \llbracket \bar{\mathbf{v}}' \rrbracket \cdot \mathbf{K}_\kappa \llbracket \hat{\mathbf{v}} \rrbracket dS. \end{aligned} \quad (64)$$

Subtracting (63) from (64), one finds

$$\begin{aligned} -\langle T_\kappa \mathbf{X}, \mathbf{X}' \rangle &= \int_{\mathcal{D}_\kappa^* \setminus \overline{\Gamma_\kappa}} \nabla (\bar{\mathbf{u}}' + \bar{\mathbf{v}}') : (\mathbf{C}_\kappa - \mathbf{C}) : \nabla (\hat{\mathbf{u}} + \hat{\mathbf{v}}) dV + \int_{\mathcal{B}_\kappa^- \cup \mathcal{D}_\kappa^* \setminus \overline{\Gamma_\kappa}} \nabla \bar{\mathbf{v}}' : \mathbf{C} : \nabla \hat{\mathbf{v}} dV - \\ & - \int_{\Gamma_\kappa \cap \overline{\mathcal{D}_\kappa^*}} [\mathbf{t}[\hat{\mathbf{u}}] \cdot \llbracket \bar{\mathbf{v}}' \rrbracket + \bar{\mathbf{t}}[\mathbf{u}'] \cdot \llbracket \hat{\mathbf{v}} \rrbracket] dS - \int_{\Gamma_\kappa \setminus \overline{\mathcal{D}_\kappa^*}} [\boldsymbol{\psi} \cdot \llbracket \bar{\mathbf{v}}' \rrbracket + \bar{\boldsymbol{\psi}}' \cdot \llbracket \hat{\mathbf{v}} \rrbracket] dS - \\ & - \int_{\partial \mathcal{D}_\kappa^o} [\boldsymbol{\phi} \cdot \bar{\mathbf{v}}' + \bar{\boldsymbol{\phi}}' \cdot \hat{\mathbf{v}} + \bar{\boldsymbol{\phi}}' \cdot \hat{\mathbf{u}}_\phi] dS + \int_{\Gamma_\kappa} \llbracket \bar{\mathbf{v}}' \rrbracket \cdot \mathbf{K}_\kappa \llbracket \hat{\mathbf{v}} \rrbracket dS + \\ & + \int_{\mathcal{D}_\kappa^* \setminus \overline{\Gamma_\kappa}} \omega^2 (\rho - \rho_\kappa) (\bar{\mathbf{u}}' + \bar{\mathbf{v}}') \cdot (\hat{\mathbf{u}} + \hat{\mathbf{v}}) dV - \int_{\mathcal{B}_\kappa^- \cup \mathcal{D}_\kappa^* \setminus \overline{\Gamma_\kappa}} \rho \omega^2 \bar{\mathbf{v}}' \cdot \hat{\mathbf{v}} dV, \end{aligned} \quad (65)$$

On the other hand, adding (63) to (64), the result can be recast as

$$\begin{aligned} \langle T_\kappa \mathbf{X}, \mathbf{X}' \rangle &= \int_{\mathcal{D}_\kappa^* \setminus \overline{\Gamma_\kappa}} \nabla \bar{\mathbf{u}}' : (\mathbf{C} - \mathbf{C}_\kappa) : \nabla \hat{\mathbf{u}} dV + \int_{\mathcal{D}_\kappa^* \setminus \overline{\Gamma_\kappa}} \nabla \bar{\mathbf{v}}' : \mathbf{C}_\kappa : \nabla \hat{\mathbf{v}} dV + \\ & \int_{\mathcal{D}_\kappa^* \setminus \overline{\Gamma_\kappa}} [\nabla \bar{\mathbf{u}}' : (\mathbf{C} - \mathbf{C}_\kappa) : \nabla \hat{\mathbf{v}} dV - \nabla \bar{\mathbf{v}}' : (\mathbf{C} - \mathbf{C}_\kappa) : \nabla \hat{\mathbf{u}}] dV + \int_{\mathcal{B}_\kappa^-} \nabla \bar{\mathbf{v}}' : \mathbf{C} : \nabla \hat{\mathbf{v}} dV + \\ & + \int_{\Gamma_\kappa \cap \overline{\mathcal{D}_\kappa^*}} [\bar{\mathbf{t}}[\mathbf{u}'] \cdot \llbracket \hat{\mathbf{v}} \rrbracket - \mathbf{t}[\hat{\mathbf{u}}] \cdot \llbracket \bar{\mathbf{v}}' \rrbracket] dS + \int_{\Gamma_\kappa \setminus \overline{\mathcal{D}_\kappa^*}} [\bar{\boldsymbol{\psi}}' \cdot \llbracket \hat{\mathbf{v}} \rrbracket - \boldsymbol{\psi} \cdot \llbracket \bar{\mathbf{v}}' \rrbracket] dS + \\ & + \int_{\partial \mathcal{D}_\kappa^o} [\bar{\boldsymbol{\phi}}' \cdot (\hat{\mathbf{u}}_\phi + \hat{\mathbf{v}}) - \boldsymbol{\phi} \cdot \bar{\mathbf{v}}'] dS + \int_{\Gamma_\kappa} \llbracket \bar{\mathbf{v}}' \rrbracket \cdot \mathbf{K}_\kappa \llbracket \hat{\mathbf{v}} \rrbracket dS - \\ & - \int_{\mathcal{D}_\kappa^* \setminus \overline{\Gamma_\kappa}} \omega^2 (\rho - \rho_\kappa) (\bar{\mathbf{u}}' - \bar{\mathbf{v}}') \cdot (\hat{\mathbf{u}} + \hat{\mathbf{v}}) - \int_{\mathcal{B}_\kappa^- \cup \mathcal{D}_\kappa^* \setminus \overline{\Gamma_\kappa}} \rho \omega^2 \bar{\mathbf{v}}' \cdot \hat{\mathbf{v}} dV. \end{aligned} \quad (66)$$

In light of (65) and (66), define $T_{\circ}^{\pm}: \mathfrak{S}(H_{\Delta}) \rightarrow \tilde{S}(\mathcal{D}_{\kappa}^* \cup \Gamma_{\kappa} \cup \partial\mathcal{D}_{\kappa}^o)$ such that

$$\begin{aligned} -\langle T_{\circ}^{-} \mathbf{X}, \mathbf{X}' \rangle &= \int_{\mathcal{D}_{\kappa}^* \setminus \overline{\Gamma_{\kappa}}} \nabla(\bar{\mathbf{u}}' + \bar{\mathbf{v}}') : (\mathbf{C}_{\kappa} - \mathbf{C}) : \nabla(\hat{\mathbf{u}} + \hat{\mathbf{v}}) dV + \\ &+ \int_{\mathcal{D}_{\kappa}^- \cup \mathcal{D}_{\kappa}^* \setminus \overline{\Gamma_{\kappa}}} \nabla \bar{\mathbf{v}}' : \mathbf{C} : \nabla \hat{\mathbf{v}} dV + \int_{\mathcal{D}_{\kappa}^* \setminus \overline{\Gamma_{\kappa}}} \bar{\mathbf{u}}' \cdot \hat{\mathbf{u}} dV, \end{aligned} \quad (67)$$

$$\begin{aligned} \langle T_{\circ}^{+} \mathbf{X}, \mathbf{X}' \rangle &= \int_{\mathcal{D}_{\kappa}^* \setminus \overline{\Gamma_{\kappa}}} \nabla \bar{\mathbf{u}}' : (\mathbf{C} - \mathbf{C}_{\kappa}) : \nabla \hat{\mathbf{u}} dV + \int_{\mathcal{D}_{\kappa}^* \setminus \overline{\Gamma_{\kappa}}} \nabla \bar{\mathbf{v}}' : \mathbf{C}_{\kappa} : \nabla \hat{\mathbf{v}} dV + \\ &+ \int_{\mathcal{D}_{\kappa}^* \setminus \overline{\Gamma_{\kappa}}} [\nabla \bar{\mathbf{u}}' : (\mathbf{C} - \mathbf{C}_{\kappa}) : \nabla \hat{\mathbf{v}} dV - \nabla \bar{\mathbf{v}}' : (\mathbf{C} - \mathbf{C}_{\kappa}) : \nabla \hat{\mathbf{u}}] dV + \\ &+ \int_{\mathcal{B}_{\kappa}^-} \nabla \bar{\mathbf{v}}' : \mathbf{C} : \nabla \hat{\mathbf{v}} dV + \int_{\mathcal{D}_{\kappa}^* \setminus \overline{\Gamma_{\kappa}}} \bar{\mathbf{u}}' \cdot \hat{\mathbf{u}} dV. \end{aligned} \quad (68)$$

Given Assumption 4.2, it is evident that $\Re(e^{i\theta} T_{\circ}^{-})$ is coercive on $\mathfrak{S}(H_{\Delta})$ for $\theta = [0, \pi/2)$ provided that the first of Assumption 4.3 holds. In the second case of the latter, however, one may show that $\Re(T_{\circ}^{+})$ is coercive on $\mathfrak{S}(H_{\Delta})$ by following the argument used in the proof of [18, Theorem 2.47]. Now, by deploying the Rellich compact embeddings along with the regularity of the trace operator, one concludes that

$$T_c := \Re(T_{\kappa} - T_{\circ}^{\pm}): \mathfrak{S}(H_{\Delta}) \rightarrow \tilde{S}(\mathcal{D}_{\kappa}^* \cup \Gamma_{\kappa} \cup \partial\mathcal{D}_{\kappa}^o)$$

is compact.

References

- [1] M. G. Amin. *Through-the-wall radar imaging*. CRC press, 2017.
- [2] Jorge F Arinez, Qing Chang, Robert X Gao, Chengying Xu, and Jianjing Zhang. Artificial intelligence in advanced manufacturing: Current status and future outlook. *Journal of Manufacturing Science and Engineering*, 142(11), 2020.
- [3] J. D. Arregui-Mena, T. Koyanagi, E. Cakmak, C. M. Petrie, W.-J. Kim, D. Kim, C. P. Deck, C. Sauder, J. Braun, and Y. Katoh. Qualitative and quantitative analysis of neutron irradiation effects in sic/sic composites using x-ray computed tomography. *Composites Part B: Engineering*, 238:109896, 2022.
- [4] C. Atkinson. On stress singularities and interfaces in linear elastic fracture mechanics. *International Journal of Fracture*, 13(6):807–820, 1977.
- [5] L. Audibert, L. Chesnel, H. Haddar, and K. Napal. Qualitative indicator functions for imaging crack networks using acoustic waves. *SIAM Journal on Scientific Computing*, 43(2):B271–B297, 2021.

- [6] L. Audibert, A. Girard, and H. Haddar. Identifying defects in an unknown background using differential measurements. *Inverse Probl. Imaging*, 9(3), 2015.
- [7] L. Audibert and H. Haddar. The generalized linear sampling method for limited aperture measurements. *SIAM Journal on Imaging Sciences*, 10(2):845–870, 2017.
- [8] Chaitanya Bakre, Seyed Hamidreza Afzalimir, Cory Jamieson, Abdalla Nassar, Edward W Reutzel, and Cliff J Lissenden. Laser generated broadband rayleigh waveform evolution for metal additive manufacturing process monitoring. *Applied Sciences*, 12(23):12208, 2022.
- [9] O. I. Balitskii, Y. H. Kvasnytska, L. M. Ivaskevych, H. P. Mialnitsa, and K. H. Kvasnytska. Fatigue fracture of the blades of gas-turbine engines made of a new refractory nickel alloy. *Materials Science*, 57(4):475–483, 2022.
- [10] G. I. Barenblatt. *Scaling (Cambridge texts in applied mathematics)*. Cambridge University Press, Cambridge, UK, 2003.
- [11] P. W. R. Beaumont. Slow cracking in composite materials: Catastrophic fracture of composite structures. In *The Structural Integrity of Carbon Fiber Composites*, pages 489–528. Springer, 2017.
- [12] C. Bellis, F. Cakoni, and B. B. Guzina. Nature of the transmission eigenvalue spectrum for elastic bodies. *The IMA Journal of Applied Mathematics*, 78(5):895–923, 2013.
- [13] C. Bellis and B. B. Guzina. On the existence and uniqueness of a solution to the interior transmission problem for piecewise-homogeneous solids. *Journal of Elasticity*, 101(1):29–57, 2010.
- [14] L. J. Bond. Needs and opportunities: nondestructive evaluation for energy systems. In *Smart Materials and Nondestructive Evaluation for Energy Systems 2015*, volume 9439, page 943902. International Society for Optics and Photonics, 2015.
- [15] M Bonnet. *Boundary integral equations methods for solids and fluids*. Wiley, 1999.
- [16] M. Bonnet and F. Cakoni. Analysis of topological derivative as a tool for qualitative identification. *Inverse Problems*, 35(10):104007, 2019.
- [17] Anton Bychkov, Varvara Simonova, Vasily Zarubin, Elena Cherepetskaya, and Alexander Karabutov. The progress in photoacoustic and laser ultrasonic tomographic imaging for biomedicine and industry: A review. *Applied Sciences*, 8(10):1931, 2018.
- [18] F. Cakoni, D. Colton, and H. Haddar. *Inverse scattering theory and transmission eigenvalues*. Society for Industrial and Applied Mathematics, 2016.
- [19] F. Cakoni, D. Colton, and H. Haddar. A duality between scattering poles and transmission eigenvalues in scattering theory. *Proceedings of the Royal Society A*, 476(2244):20200612, 2020.

- [20] F. Cakoni, P.-Z. Kow, and J.-N. Wang. The interior transmission eigenvalue problem for elastic waves in media with obstacles. *Inverse Problems & Imaging*, 15(3):445, 2021.
- [21] Sergio Cantero-Chinchilla, Paul D Wilcox, and Anthony J Croxford. Deep learning in automated ultrasonic nde—developments, axioms and opportunities. *NDT & E International*, page 102703, 2022.
- [22] A. Charalambopoulos. On the interior transmission problem in nondissipative, inhomogeneous, anisotropic elasticity. *Journal of elasticity and the physical science of solids*, 67(2):149–170, 2002.
- [23] A. Charalambopoulos and K. A. Anagnostopoulos. On the spectrum of the interior transmission problem in isotropic elasticity. *Journal of Elasticity*, 90(3):295–313, 2008.
- [24] A. Charalambopoulos, D. Gintides, and K. Kiriaki. The linear sampling method for the transmission problem in three-dimensional linear elasticity. *Inverse Problems*, 18(3):547, 2002.
- [25] A. Charalambopoulos, A. Kirsch, K. A. Anagnostopoulos, D. Gintides, and K. Kiriaki. The factorization method in inverse elastic scattering from penetrable bodies. *Inverse Problems*, 23(1):27, 2006.
- [26] Y. Chen and L. Dal Negro. Physics-informed neural networks for imaging and parameter retrieval of photonic nanostructures from near-field data. *APL Photonics*, 7(1):010802, 2022.
- [27] Y. Chen, L. Lu, G. Em Karniadakis, and L. Dal Negro. Physics-informed neural networks for inverse problems in nano-optics and metamaterials. *Optics express*, 28(8):11618–11633, 2020.
- [28] C. Daux, N. Moës, J. Dolbow, N. Sukumar, and T. Belytschko. Arbitrary branched and intersecting cracks with the extended finite element method. *International journal for numerical methods in engineering*, 48(12):1741–1760, 2000.
- [29] S. J. Davies, C. Edwards, G. S. Taylor, and S. B. Palmer. Laser-generated ultrasound: its properties, mechanisms and multifarious applications. *Journal of Physics D: Applied Physics*, 26(3):329, 1993.
- [30] J. S. del Río, C. Pascual-Gonzalez, V. Martinez, J. L. Jiménez, and C. Gonzalez. 3d-printed resistive carbon-fiber-reinforced sensors for monitoring the resin frontal flow during composite manufacturing. *Sensors and Actuators A: Physical*, 317:112422, 2021.
- [31] José JR Faria, Luiz GA Fonseca, Alfredo R de Faria, Artur Cantisano, Thiago N Cunha, Hamid Jahed, and John Montesano. Determination of the fatigue behavior of mechanical components through infrared thermography. *Engineering Failure Analysis*, 134:106018, 2022.

- [32] SC Garcea, Ying Wang, and PJ Withers. X-ray computed tomography of polymer composites. *Composites Science and Technology*, 156:305–319, 2018.
- [33] S. Goswami and W. Becker. Computation of 3-d stress singularities for multiple cracks and crack intersections by the scaled boundary finite element method. *International journal of fracture*, 175(1):13–25, 2012.
- [34] B. B. Guzina and F. Pourahmadian. Why the high-frequency inverse scattering by topological sensitivity may work. *Proceedings of the Royal Society A: Mathematical, Physical and Engineering Sciences*, 471(2179):20150187, 2015.
- [35] P. Hähner. On the uniqueness of the shape of a penetrable, anisotropic obstacle. *Journal of computational and applied mathematics*, 116(1):167–180, 2000.
- [36] A. Kirsch and N. Grinberg. *The factorization method for inverse problems*, volume 36. Oxford University Press, 2008.
- [37] T. G. Lach, C. M. Silva, Y. Zhou, W. L. Boldman, P. D. Rack, W. J. Weber, and Y. Zhang. Dynamic substrate reactions during room temperature heavy ion irradiation of cocrcufeni high entropy alloy thin films. *npj Materials Degradation*, 6(1):1–15, 2022.
- [38] C. K. C. Lieou and C. A. Bronkhorst. Thermomechanical conversion in metals: dislocation plasticity model evaluation of the taylor-quinney coefficient. *Acta Materialia*, 202:170–180, 2021.
- [39] S. Liu, K. Jia, H. Wan, L. Ding, X. Xu, L. Cheng, S. Zhang, X. Yan, M. Lu, and G. Ma. Inspection of the internal defects with different size in ni and ti additive manufactured components using laser ultrasonic technology. *Optics & Laser Technology*, 146:107543, 2022.
- [40] K. K. Lo. Analysis of branched cracks. *Journal of Applied Mechancis*, 45(4):797–802, 1978.
- [41] C. Meier, R. Weissbach, J. Weinberg, W. A Wall, and A. J. Hart. Critical influences of particle size and adhesion on the powder layer uniformity in metal additive manufacturing. *Journal of Materials Processing Technology*, 266:484–501, 2019.
- [42] D. A. Mendelsohn. A review of hydraulic fracture modeling – ii: 3d modeling and vertical growth in layered rock. *Journal of Energy Resources Technology*, 106(4):543–553, 1984.
- [43] D. J. Mukai, R. Ballarini, and G. R. Miller. Analysis of branched interface cracks. *Journal of Applied Mechanics*, 57(4):887–893, 1990.
- [44] V. V. Narumanchi, F. Pourahmadian, J. Lum, A. Townsend, J. W. Tringe, D. M. Stobbe, and T. W. Murray. Laser ultrasonic imaging of subsurface defects with the linear sampling method. *Optics express*, 2022. under review.

- [45] U. Netzelmann, A. Mross, T. Waschkies, D. Weber, E. Toma, and H. Neurohr. Non-destructive testing of the integrity of solid oxide fuel cell stack elements by ultrasound and thermographic techniques. *Energies*, 15(3):831, 2022.
- [46] T.-P. Nguyen. Differential imaging of local perturbations in anisotropic periodic media. *Inverse Problems*, 36(3):034004, 2020.
- [47] R. Pokharel, D. W. Brown, B. Clausen, D. D. Byler, T. L. Ickes, K. J. McClellan, R. M. Suter, and P. Kenesei. Non-destructive characterization of uo_{2+x} nuclear fuels. *Microscopy Today*, 25(6):42–47, 2017.
- [48] F. Pourahmadian. Experimental validation of differential evolution indicators for ultrasonic imaging in unknown backgrounds. *Mechanical Systems and Signal Processing*, 161:108029, 2021.
- [49] F. Pourahmadian, B. B. Guzina, and H. Haddar. Generalized linear sampling method for elastic-wave sensing of heterogeneous fractures. *Inverse Problems*, 33(5):055007, 2017.
- [50] F. Pourahmadian and H. Haddar. Differential tomography of micromechanical evolution in elastic materials of unknown micro/macrostructure. *SIAM Journal on Imaging Sciences*, 13(3):1302–1330, 2020.
- [51] S. Roy, A. Kumar, and S. Li. A nano-micro-macro-multiscale model for progressive failure prediction in advanced composites. In *The Structural Integrity of Carbon Fiber Composites*, pages 137–169. Springer, 2017.
- [52] K. Terrani. Accident tolerant fuel cladding development: Promise, status, and challenges. *Journal of Nuclear Materials*, 501:13–30, 2018.
- [53] A. Van der Heijden. Developments and challenges in the manufacturing, characterization and scale-up of energetic nanomaterials – a review. *Chemical Engineering Journal*, 350:939–948, 2018.
- [54] Ruud JG Van Sloun, Regev Cohen, and Yonina C Eldar. Deep learning in ultrasound imaging. *Proceedings of the IEEE*, 108(1):11–29, 2019.
- [55] Paul D Wilcox, Anthony J Croxford, Nicolas Budyn, Rhodri LT Bevan, Jie Zhang, Artem Kashubin, and Peter Cawley. Fusion of multi-view ultrasonic data for increased detection performance in non-destructive evaluation. *Proceedings of the Royal Society A*, 476(2243):20200086, 2020.
- [56] G. Yan, S. Raetz, N. Chigarev, V. E. Gusev, and V. Tournat. Characterization of progressive fatigue damage in solid plates by laser ultrasonic monitoring of zero-group-velocity lamb modes. *Physical Review Applied*, 9(6):061001, 2018.

- [57] Jie Zhang, Xudong Niu, Anthony J Croxford, and Bruce W Drinkwater. Strategies for guided acoustic wave inspection using mobile robots. *Proceedings of the Royal Society A*, 478(2259):20210762, 2022.
- [58] Jun Zhang, Jinfeng Wu, Xin Zhao, Shuxian Yuan, Guanbing Ma, Jiaqi Li, Ting Dai, Huaidong Chen, Bing Yang, and Hui Ding. Laser ultrasonic imaging for defect detection on metal additive manufacturing components with rough surfaces. *Applied Optics*, 59(33):10380–10388, 2020.
- [59] X. Zhang, J. R. Fincke, C. M. Wynn, M. R. Johnson, R. W. Haupt, and B. W. Anthony. Full noncontact laser ultrasound: first human data. *Light: Science & Applications*, 8(1):1–11, 2019.
- [60] Qihan Zhao, Xizuo Dan, Fangyuan Sun, Yonghong Wang, Sijin Wu, and Lianxiang Yang. Digital shearography for ndt: phase measurement technique and recent developments. *Applied Sciences*, 8(12):2662, 2018.
- [61] R. Zimmermann, E. Mohseni, D. Lines, R. K. W. Vithanage, C. N. MacLeod, S. G. Pierce, A. Gachagan, Y. Javadi, S. Williams, and J. Ding. Multi-layer ultrasonic imaging of as-built wire+ arc additive manufactured components. *Additive Manufacturing*, 48:102398, 2021.